BANK OF CANADA
BANQUE DU CANADA

Staff Discussion Paper/Document d'analyse du personnel—2022-6

Last updated: March 22, 2022

Real Exchange Rate Decompositions

by Bruno Feunou, Jean-Sébastien Fontaine and Ingomar Krohn

Financial Markets Department
Bank of Canada

BFeunou@bankofcanada.ca
jsfontaine@bankofcanada.ca
IKrohn@bankofcanada.ca

DOI: https://doi.org/10.34989/sdp-2022-6 | **ISSN** 1914-0568

Acknowledgements

We are grateful to Larry Schembri, Antonio Diez de los Rios, Geoffrey Dunbar, Jonathan Witmer, James Kyeong and Andreas Uthemann for their comments and suggestions. We also thank seminar participants and colleagues from the Financial Markets Department for insightful discussions.

Abstract

We provide a novel daily decomposition of the real exchange rate that exploits a direct link between bond and foreign exchange (FX) markets. Real exchange rate dynamics can be attributed to changes in the expected future level of the exchange rate; cross-country differentials of expected inflation, yields and bond term premia; and an FX risk premium. Through a variance decomposition exercise, we find that the FX risk premium is the dominant component. Monetary policies and macroeconomic news announcements largely move the real exchange through changes in the FX risk premium.

Topics: Asset pricing, Exchange rates, International financial markets, Monetary policy transmission
JEL codes: E43, F31, G12

1 Introduction

In principle, the exchange rate is one of the main transmission channels of monetary policies in Canada, directly affecting the value of the Canadian dollar vis-à-vis the US dollar through the countries' interest rate differential. For example, a drop in Canadian interest rates *may* lead to a weaker Canadian dollar, translating into higher prices for imported goods and services, while at the same time locally produced goods, based on comparably lower domestic prices, become more attractive in foreign markets and boost global exports. As is well documented in the literature (see, e.g., Meese and Rogoff 1983, Engel 2013), however, exchange rates appear to be largely disconnected from interest rate differentials and other macroeconomic fundamentals, suggesting that the transmission channel of monetary policy and macroeconomic news is not straightforward but rather complex; thus, a change in interest rates does not necessarily map one to one into an expected change in the exchange rate.

Our objectives in this paper are to quantify the exchange rate transmission channel and to explore a variety of policy-relevant questions: To what extent does the exchange rate transmission channel work? That is, does a drop in Canadian interest rates (relative to interest rate levels in the United States) lead to a depreciation of the Canadian dollar? Or conversely, to what degree does a hawkish monetary policy decision lead to a stronger Canadian dollar vis-à-vis the US dollar? What is the magnitude of this transmission relative to factors outside of bond markets, and does the (in)efficiency of monetary policy transmission depend on where changes along the yield curve take place?

To address these questions, we derive a daily accounting identity for the real exchange rate based on the well-known uncovered interest parity (UIP) condition (Engel and West 2005). We show that the exchange rate between the Canadian dollar and the US dollar on any given day can be expressed as the sum of (1) the expectation of future spot rate levels, (2) the expected inflation differential, (3) the difference between Government of Canada bonds and US Treasury yields, (4) the Canadian and US term premia differential and (5) a foreign exchange rate risk premium. These components do not evolve independently of each other, i.e., the same or related economic forces may affect one or all of the real exchange rate components concurrently. These contemporaneous interrelations between factors may explain why changes in the interest rate differential (between

Canada and the United States) do not necessarily translate into the expected changes in the values of the exchange rate—or why, when the expected changes do happen, the transmission is only partial.

To illustrate the need for a model that enables researchers and policy-makers to quantify components of the real exchange rate, consider the correlation between the real CAD-USD exchange rate and the countries' interest rate differentials. The sample correlations for the period following the 2007–08 global financial crisis, from 2008 to 2021, are high and **positive** (0.86 and 0.66 for the 2- and 10-year maturity), suggesting that on average an increase in the Canadian interest rate relative to that of the United States is associated with an appreciation of the Canadian dollar. This intuitive exchange rate response hides some significant time series variation. In Chart (1), we plot the rolling window correlation, which depicts interesting insights. There are substantial variations in the correlation between the exchange rate and interest rate differentials, which are positive and high most of the time but can be negative and have recently hovered around -0.5. This negative exchange rate response is in line with a large empirical literature on UIP failure (Fama 1984*b*), documenting that short-term interest rates and currency spot returns tend to move in directions that are the opposite of what theory would suggest (see, e.g., Engel 1996, Engel 2013).[1] The weak empirical evidence of UIP indicates the interest rate differential is correlated with components of the CAD-USD exchange rate that dominate the monetary policy transmission channel and drive the overall direction of the exchange rates' response. To provide suggestive evidence, we find that the correlation between the interest rate differentials and the foreign exchange (FX) risk premium has recently turned **positive** and is now hovering around 0.5. This positive correlation implies that an increase in the Canadian interest rate relative to that of the United States pushes up the expected return on a strategy that borrows in US dollars and invests in the Canadian dollar. Consequently, the Canadian dollar depreciates.

To derive a daily exchange rate decomposition, we exploit the variation in the daily real exchange rate and the cross-section of nominal and real bond market dynamics. Importantly, instead of focusing solely on the short-term interest rate spread between two countries, we extract five factors from the entire nominal and real differential curve and one factor from the exchange rate. Then

[1] On the relationship between long-term yields and UIP, see, e.g., Chinn and Meredith 2004.

we embed these factors within a classic vector autoregressive (VAR) framework, which allows us to track and model the dynamics of the factor decomposition. Embedding the real exchange and its components in a VAR framework allows us to quantify the impact of monetary policy shocks and macroeconomic news surprises on the individual components in our exchange rate accounting identity.

We find that a surprise tightening of the monetary stance by the Bank of Canada generally results in a significant appreciation of Canadian dollars relative to the US dollar. That appreciation is distributed equally between an expectation of a future appreciation and a drop in the returns of a strategy that borrows in USD and invests in CAD. We also find that communication about the Bank of Canada's future interest rate decisions affects the exchange rate mainly through the FX risk premium channel. Similarly, macroeconomic news largely drives exchange rate dynamics through changes in expectations about the future spot rate and the FX risk premium. In contrast, yield factors and bond market term premia appear to be comparably more sticky and react less strongly to central bank and macroeconomic news.

This paper proceeds as follows. Section 2 introduces the accounting identity of the real exchange rate that is the basis of our decomposition. Section 3 describes the model and the estimation procedure, while Section 4 provides a brief overview of the data. Section 5 discusses summary statistics, documents time series dynamics of the decomposed exchange rate, and presents results based on various event study exercises. Section 6 concludes.

2 Accounting decomposition of the real exchange rate

To introduce an accounting identity of the real exchange rate, we begin by considering a zero-cost strategy that borrows in US dollars and invests in a foreign currency, e.g., Canadian dollars. By definition, the log excess return on this strategy is defined as the log exchange rate appreciation plus the interest rate differential:

$$r_{t+1} = s_{t+1} - s_t + i_t^* - i_t, \tag{1}$$

where s_t is the nominal exchange rate in dollars per unit of foreign currency at date t, and i_t and i_t^* are the US and foreign interest rates between t and $t+1$, respectively. We refer to r_{t+1} as a currency return and to the conditional expectation of it, $E_t[r_{t+1}]$, as the expected currency return or the currency risk premium.

UIP states that the nominal exchange rate should, in expectation, move to compensate exactly for any difference in interest rates and that the currency risk premium should be zero, i.e., $E_t[s_{t+1} - s_t] = -(i_t^* - i_t)$ and $E_t[r_{t+1}] = 0$. This is typically evaluated by regressing the change in the exchange rate on the lagged interest rate differential (Fama 1984*a*):

$$s_{t+1} - s_t = \alpha - \beta(i_t^* - i_t) + \varepsilon_{t+1}, \tag{2}$$

where ε_{t+1} is an error term that is assumed to be uncorrelated with all available information at date t (in particular, uncorrelated with the interest rate differential). UIP implies that $\beta = 1$, which is routinely rejected in the data. In fact, as shown by a vast literature, the estimates of the β coefficient are frequently found to be smaller than one and often even negative. A negative β means that a currency with a relatively high interest rate tends to appreciate against the dollar, while UIP implies that it should instead depreciate. This empirical finding is often referred to as the UIP (or forward premium) puzzle.[2]

In a next step, we add the interest rate differential, $i_t^* - i_t$, to both sides of (2) to obtain:

$$r_{t+1} = \alpha + (1-\beta)(i_t^* - i_t) + \varepsilon_{t+1}. \tag{3}$$

The general interpretation of $\beta < 1$ in the literature is that currency risk premia are time varying and positively correlated with interest rate differentials, and asset pricing models often assume a perfect one to one comovement between both factors (see, e.g., Backus, Foresi and Telmer 2001; Verdelhan 2010; Farhi and Gabaix 2015). We relax that assumption in our model.

First, we express Equation (1) in terms of real variables, such that

$$r_{t+1} = q_{t+1} - q_t + i_t^* - i_t - \left(\pi_{t+1}^* - \pi_{t+1}\right), \tag{4}$$

[2]Comprehensive surveys of the literature are provided, for example, in Engel (1996) or Engel (2013).

where $q_t = s_t + p_t^* - p_t$ is the real exchange rate, and $\pi_{t+1} = p_{t+1} - p_t$ and $\pi_{t+1}^* = p_{t+1}^* - p_t^*$ are the domestic and foreign inflation rates between t and $t+1$, respectively. Second, we rearrange (4), write it in terms of the real exchange rate, iterate forward and take conditional expectations as in Engel and West (2005):

$$q_t = E_t\left[q_{t+m}\right] - \sum_{j=1}^{m} E_t\left[\pi_{t+j}^* - \pi_{t+j}\right] + \sum_{j=0}^{m-1} E_t\left[i_{t+j}^* - i_{t+j}\right] - \sum_{j=1}^{m} E_t\left[r_{t+j}\right]. \tag{5}$$

Equation (5) implies that an appreciation of the foreign currency is related to either (1) an expectation of a future appreciation, (2) an expected decrease in the foreign inflation rate relative to domestic price levels, (3) an expected relative tightening of the foreign monetary policy or (4) a decrease of the FX risk premium.

Furthermore, utilizing the fact that the nominal yield is the sum of the expected short rate and the term premium, Equation 5 can be further decomposed into

$$q_t = E_t\left[q_{t+m}\right] - \sum_{j=1}^{m} E_t\left[\pi_{t+j}^* - \pi_{t+j}\right] + m\left(y_t^{(m*)} - y_t^{(m)}\right) - m\left(TP_t^{(m*)} - TP_t^{(m)}\right) - \sum_{j=1}^{m} E_t\left[r_{t+j}\right], \tag{6}$$

where $y_t^{(m*)}$ and $y_t^{(m)}$ denote the zero-coupon yield at maturity m for the home and foreign government, respectively; $TP_t^{(m*)}$ and $TP_t^{(m)}$ are the corresponding term premia. In contrast to the previous accounting identity, Equation (6) implies that an appreciation of the foreign currency can also be attributed to either an increase of the long-term cost of borrowing in the foreign country relative to the home country, or a decrease of the perceived riskiness of longer-term securities in the foreign country relative to the home country.

Another important implication of Equation (6) is that over a long horizon, the risk premium entails two components: (1) the difference between additional returns that lenders demand for holding a longer-term foreign bond instead of investing in a series of short-term foreign securities and additional returns for holding a longer-term bond in the home country instead of investing in a series of short-term securities (i.e., the term premium differential), and (2) the additional returns that investors require when borrowing in their home currency and investing in a foreign currency every period. We expect the latter component to dominate in the short run as term premia are in general negligible for short-maturity securities, but in the long run, the term premium differential

should be the dominant component.

Lastly, using the fact that the break-even inflation rate (denoted by $ISR_t^{(m)}$) is the sum of the expected average inflation between period t and $t+m$ and the so-called inflation risk premium (denoted by $IRP_t^{(m)}$), Equation (6) can be further decomposed into

$$\begin{aligned} q_t &= E_t\left[q_{t+m}\right] - m\left(ISR_t^{(m*)} - ISR_t^{(m)}\right) + m\left(y_t^{(m*)} - y_t^{(m)}\right) \\ &\quad + m\left(IRP_t^{(m*)} - IRP_t^{(m)}\right) - m\left(TP_t^{(m*)} - TP_t^{(m)}\right) - \sum_{j=1}^{m} E_t\left[r_{t+j}\right]. \end{aligned} \tag{7}$$

The following observations are worth highlighting. First, the quantities on the right-hand side of Equations (5) to (7) are correlated among each other and driven by a small set of factors. Second, these correlations explain the muted (and most of the time counterintuitive) exchange rate transmission channel of monetary policies, i.e., the decomposition allows depiction of which quantities of the right-hand side move in expected and unexpected directions, following monetary and macroeconomic news announcements. Lastly, most of the quantities are not directly observable at all or at least not at the daily frequency; thus, they must be derived from a model that links the interactions between the right-hand side variables. The objective of the next section is to outline the model structure and dynamics.

3 Model

3.1 The cross-section of the yield curve differential

With the objective in mind to model the quantities and their correlations of Equations (5) to (7), we build up the foundation of our model, noting that a small number of factors is sufficient to describe how interest rate differentials vary with the maturity m. Hence, we assume that

$$y_t^{(m*)} - y_t^{(m)} = b_m' X_t. \tag{8}$$

We verify this assertion by performing a simple principal component analysis that reveals that X_t is a 3×1 vector. Furthermore, following the seminal work by Nelson and Siegel (1987), we impose

the following structure on b_m:

$$b_m' = \left(\begin{array}{ccc} 1 & \frac{1-e^{-\lambda m}}{\lambda m} & \frac{1-e^{-\lambda m}}{\lambda m} - e^{-\lambda m} \end{array} \right), \tag{9}$$

which implies that the components of X_t are interpreted as level, slope and curvature of the yield curve differential. Chen and Tsang (2013) use the same structure to show that the yield curve differential predicts exchange rates and movements of the exchange rate risk premia.

3.2 The cross-section of the inflation-swap curve differential

Next, we note that a small number of factors is sufficient to describe how inflation swap rate differentials vary with maturity m. Hence, we assume that

$$ISR_t^{(m,*)} - ISR_t^{(m)} \quad = \quad c_m' X_t + w_m' Z_t = \bar{c}_m' \bar{X}_t, \tag{10}$$

where $\bar{X}_t' \equiv (X_t', Z_t')$ and $\bar{c}_m \equiv (c_m, w_m)$. The interpretation of these dynamics is the following. First, the nominal yield curve factor X_t can explain some–though not all–of the cross-sectional variation in the inflation swap differential between the foreign and domestic country. Second, some information in the cross-section of inflation swaps is not spanned by the nominal curve. This additional information is spanned by Z_t.

3.3 The foreign exchange rate risk premium

We assume that the cross-sections of both the nominal yield and inflation swap rate differentials are useful to predict the exchange rate excess return; that is:

$$E_t\left[r_{t+1}\right] \quad = \quad \alpha + \beta' X_t + \varphi' Z_t + \eta_t = \alpha + \bar{\beta}' \bar{X}_t + \eta_t, \tag{11}$$

where $\bar{\beta} \equiv (\beta, \varphi)'$. Equation (11) implies that the nominal yield and inflation swap curves are not enough to predict the exchange rate excess return, and additional factors might improve the model fit. We denote that additional factor by η_t. In that sense, we follow Dahlquist and Pénasse (2022), who label η_t the "missing risk premium." In fact, in our derivations below, we show how to recover η_t from the real exchange rate q_t; this means that the exchange rate and information in both the

nominal yield and inflation swap rate curves are used to forecast the exchange rate excess return.

3.4 The dynamic for X_t, Z_t and η_t

We use the following VAR(1) process, augmented with η_t, to forecast X_{t+1} and Z_{t+1}:

$$E_t\left[\bar{X}_{t+1}\right] = K_0 + \Phi\bar{X}_t + \eta_t\gamma. \tag{12}$$

We also assume that the missing risk premium factor η_t follows a univariate autoregressive (AR(1)) process,

$$E_t\left[\eta_{t+1}\right] = \lambda_\eta\eta_t. \tag{13}$$

3.5 The inflation risk premium

To complete the model, we assume that the one-step-ahead inflation risk premium (differential) is constant; that is

$$\begin{aligned} E_t\left[\pi^*_{t+1} - \pi_{t+1}\right] &= ISR^{(1*)}_t - ISR^{(1)}_t + \mu_\pi \\ &= \mu_\pi + c_1'X_t + w_1'Z_t = \mu_\pi + \bar{c}_1'\bar{X}_t, \end{aligned} \tag{14}$$

where $\bar{c}_1 = (c_1, w_1)'$. It is a fairly uncontroversial assumption as it is well established that the expectation hypothesis holds at very short maturities, and Equation (14) enables us to compute the inflation expectation at any horizon.

3.6 Model implications

We show that the model components laid out in Equations (8) to (14), in combination with the accounting decomposition of q_t given in Equation (5), imply that

$$\begin{aligned} q_t &= E_t\left[q_{t+m}\right] - m\mu_\pi - m\alpha + m\left(\bar{b}_1 - \bar{c}_1 - \bar{\beta}\right)'\mu_X \\ &\quad + \left(\bar{b}_1 - \bar{c}_1 - \bar{\beta}\right)'\tilde{\Phi}_m\left(\bar{X}_t - \mu_X\right) + \left(\left(\bar{b}_1 - \bar{c}_1 - \bar{\beta}\right)'\tilde{\gamma}_m - \tilde{\lambda}^{(m)}_\eta\right)\eta_t, \end{aligned} \tag{15}$$

where $\mu_X = (I - \Phi)^{-1} K_0$ is the unconditional mean of $\bar{X}_t$, and

$$\tilde{\lambda}_\eta^{(m)} \equiv \frac{1 - \lambda_\eta^m}{1 - \lambda_\eta}, \quad \tilde{\Phi}_m \equiv (I - \Phi^m)(I - \Phi)^{-1}, \quad \tilde{\gamma}_m \equiv \left(\tilde{\lambda}_\eta^{(m)} I - \tilde{\Phi}_m\right)(\lambda_\eta I - \Phi)^{-1} \gamma. \tag{16}$$

Hence, by setting

$$\mu_\pi = \left(\bar{b}_1 - \bar{c}_1 - \bar{\beta}\right)' \mu_X - \alpha, \tag{17}$$

in Equation (15), we get

$$q_t = E_t[q_{t+m}] + \left(\bar{b}_1 - \bar{c}_1 - \bar{\beta}\right)' \tilde{\Phi}_m \left(\bar{X}_t - \mu_X\right) + \left(\left(\bar{b}_1 - \bar{c}_1 - \bar{\beta}\right)' \tilde{\gamma}_m - \tilde{\lambda}_\eta^{(m)}\right) \eta_t. \tag{18}$$

Next, we assume that purchasing power parity holds in the long run, or in a statistical sense that

$$\lim_{m \to \infty} E_t[q_{t+m}] = \mu_q < \infty, \tag{19}$$

and take the limit of Equation (18). As m goes to ∞ we get

$$q_t = \mu_q + \beta_{qx}' \left(\bar{X}_t - \mu_X\right) + \beta_{q\eta} \eta_t, \tag{20}$$

where

$$\beta_{qx}' \equiv \left(\bar{b}_1 - \bar{c}_1 - \bar{\beta}\right)' \tilde{\Phi}_\infty, \quad \beta_{q\eta} \equiv \left(\bar{b}_1 - \bar{c}_1 - \bar{\beta}\right)' \tilde{\gamma}_\infty - \tilde{\lambda}_\eta^{(\infty)} \tag{21}$$

$$\tilde{\lambda}_\eta^{(\infty)} \equiv \frac{1}{1 - \lambda_\eta}, \quad \tilde{\Phi}_\infty \equiv (I - \Phi)^{-1}, \quad \tilde{\gamma}_\infty \equiv \left(\tilde{\lambda}_\eta^{(\infty)} I - \tilde{\Phi}_\infty\right)(\lambda_\eta I - \Phi)^{-1} \gamma. \tag{22}$$

We use Equation (20) to infer η_t as:

$$\eta_t = \beta_{q\eta}^{-1} \left(q_t - \mu_q - \beta_{qx}' \left(\bar{X}_t - \mu_X\right)\right). \tag{23}$$

4 Data

We estimate the model, focusing on the exchange rate between the Canadian and the US dollars in the period following the global financial crisis. The majority of data is sourced from Bloomberg.

First, we obtain daily zero coupon yields for Canada and the United States for nine maturities (3-month, 6-month, 1-year, 2-year, 5-year, 10-year, 15-year, 20-year, 30-year maturities).[3] Utilizing data with varying maturities allows us to track cross-country differences across the entire yield curve, instead of focusing only on the interest rate differential between the two countries at one particular point, i.e., using either the short or long end of the curve. Second, we obtain the nominal exchange rate between the Canadian and the US dollar. We express the rate in US dollars (home currency) per Canadian dollar (foreign currency); i.e., an increase in the exchange rate (thus, positive realized returns) implies an appreciation of the CAD vis-á-vis the USD. Third, we use Canadian and US consumer price indexes (CPI Bloomberg tickers: CACPI Index and USCPI Index) to construct the real exchange rate, as described in Equation (4).

Further, we source daily break-even inflation rates (BEIR) for both countries from Bloomberg. While a large cross-section of BEIRs exists across maturities for the United States (with maturities ranging between 1 year and 30 years), the number of available data points for Canada is comparably more limited and governs our choice for the start of the sample period. To be able to construct daily BEIR differentials between the two sovereigns (see Equation (10)), we focus on the cross-section of maturities, which are published by both countries and which provide enough data points for a reasonably long time series (i.e., 10 years, 20 years, 30 years).[4] Focusing on these three maturities, we obtain a time series for the BEIRs for the period from May 8, 2008, to February 5, 2021.

Next, we collect data on the median inflation survey expectations from the Survey of Professional Forecasters and Consensus Forecasts. The data are available at a quarterly frequency, and at each point in time the survey provides the median forecast for the subsequent five quarters. Two necessary assumptions must be made to use survey expectations data in the framework of our model. First, to compute the differences in the forecasts between the two countries, we assume both surveys are published concurrently, i.e., that the US inflation survey is published on the

[3]For Canada, the Bloomberg tickers for the zero coupon yields are I00703M Index, I00706M Index, I00701Y Index, I00702Y Index, I00705Y Index, I00710Y Index, I00715Y Index, I00720Y Index and I00730Y Index. For the United States, the Bloomberg tickers are I02503M Index, I02506M Index, I02501Y Index, I02502Y Index, I02505Y Index, I02510Y Index, I02515Y Index, I02520Y Index and I02530Y Index.

[4]BEIR Bloomberg tickers for Canada are CDGGBE10 Index, CDGGBE20 Index and CDGGBE30 Index. For the United States, the tickers are USGGBE10 Index, USGGBE20 Index and USGGBE30 Index.

same day as the Canadian inflation survey forecast. Second, survey expectations concerning price changes in the current quarter are often collected and published close to the end of the ongoing quarter. Therefore, forecasters have been observing, at least to a certain degree, the current quarter's inflation dynamics, which may have an impact on their short-term inflation forecast. To account for this, we linearly adjust current-quarter forecasts and take into account the number of days that have already passed before the forecast is published. While this does not have strong implications for the decomposition, the assumption helps to discipline our model.

Lastly, to analyse the real exchange rate dynamics around monetary policy and macroeconomic announcements, we collect data from Bloomberg on all dates, expected outcomes and realized outcomes for all monetary policy and macroeconomic announcements in the United States and Canada. In addition, we utilize high-frequency data from the Montreal Exchange on short- and long-dated Canadian Bankers' Acceptance (BAX) futures to measure the immediate response of money market rates to monetary policy statements by the Bank of Canada.

5 Results

This section presents the main empirical results and provides various applications of the exchange rate decomposition for informing policy decisions. First, we discuss some model properties, data summary statistics and the corresponding model-implied observations. Second, we document the time-series dynamics of the real exchange rate and its components. Third, we conduct a variety of event studies to document how exchange rate components behave on monetary policy announcement days and in response to macroeconomic news releases.

5.1 Model properties and summary statistics

This section discusses the empirical implications of some of the underlying assumptions that we impose to decompose the daily real exchange rate into its different components in the period following the global financial crisis. To begin with, Chart 2 documents the time series dynamics of the (real) exchange rate (left y-axis), and the three-month short-term interest rate differential (right y-axis). While the real exchange rate is largely stable across the sample period, we note the interest rate differential appears to be more volatile. In particular in the period after 2015, the interest

rate differential declines noticeably and even turns negative by 2017, while the real exchange rate dynamics are comparably muted over the same time horizon. Similarly, large swings in the interest rate differential during the crisis or during the onset of the COVID-19 pandemic appear not to be translated directly one to one into relatable exchange rate responses. The exchange rate accounting identity may provide insights into this apparent disconnect.

Next we provide some summary statistics on the model components. First, in contrast to models in previous studies, our model does not only account for the short-end dynamics of the yield differentials, but also utilizes the entire term structure. In fact, it models the connection between the bond and FX markets and builds on the well-known property that three bond market factors–level, slope and curvature–are sufficient to describe the dynamics of the yield curve differential. For example, the adjusted R^2s for regressions of yield differentials on the three factors (X_t) range between 57% (for a 10-year maturity) and 100% (for maturities of 3 months, 5 years and 30 years).[5] Further, the average annualized root mean square error over the period is only 0.18%, confirming that the three-factor model accurately captures dynamics in the bond markets across the curve.

Next, moving to the cross-section of inflation swap spreads, we document a significant relationship between X_t and the differential of countries' break-even inflation rates (for more detail, see section 7.1.2. The link between the three factors and the cross-section of BEIRs is primarily driven by the level factor, while slope and curvature factors appear to be unrelated to the cross-sectional variation of BEIRs. The average correlation between the level of the nominal rate differential and the BEIR differential is about 0.5. By construction, adding two other factors, Z_t, which are extracted from the residuals of the regression of BEIRs on X_t, yields an almost perfect fit for the cross-section of BEIR spreads.

Further, we assess the extent to which richer model dynamics (i.e., accounting for the cross-section of nominal yields and inflation swaps) helps predict the exchange rate excess returns. In other words, we are evaluating Equation (11) of the model. To do that, we regress the difference between the realized exchange rate excess return in period $t+1$ and the model-implied missing risk premium ($r_{t+1} - \eta_t$) on components of the nominal and real yield curve differentials. The

[5]The adjusted R^2s are obtained from regressing the observed yield differential (SY) at each maturity m on the three-factor model-implied yield differential (X), i.e., $SY_t^m = \alpha + \beta X_t + \varepsilon_t$. The results are not tabulated.

regression results are reported in Table 1 for daily, monthly and quarterly data, and we compare the outcomes for the full model ("Full") and different benchmark models ("BM1" and "BM2") outlined in Section 7.2. Across sampling frequencies, the Full columns refer to the model that encompasses all nominal yield factors as well as the factors capturing information from a cross-section of the inflation swaps. The BM1 columns consider only nominal yield factors, and the BM2 columns consider only information from the short-term interest rate differential, similar to the model in Dahlquist and Pénasse (2022).

Starting at the daily frequency, Table 1 confirms that predicting daily exchange rate dynamics is notoriously difficult as reflected by the low $\bar{R}^2$; yet, using the full model specification adds some explanatory power to the model. In particular, when considering the richer model that accounts for cross-sectional dynamics of yields and inflation swaps (column 1), we find that the level and slope of the break-even inflation rates are significantly and positively associated with model-implied exchange rate excess returns. The adjusted R^2 is 0.36%, while the adjusted goodness-of-fit is barely distinguishable from zero or is even negative when, respectively, only bond market factors or only the short-rate are employed as regressors. Moving on to lower frequencies, similar patterns emerge, suggesting the importance of the additional yield curve factors to explain exchange rate dynamics. At the monthly level, the goodness-of-fit of the richest model is 5.4% compared with 1.99% and -0.37% of the benchmark cases.

An immediate conclusion is that the entire yield curve differential (and not just the short end of the curve) is informative about the FX risk premium. To confirm this, we filter the "missing risk premium" (η_t) from the BM2 model and investigate the extent to which its information content is subsumed in the nominal and real yield curve differentials. We regress the missing risk premium obtained from BM2 on X_t and Z_t and report the results in Table 2. The significant coefficient estimates and moderately high adjusted R^2 across all frequencies highlight that nominal and real slope and curvature factors contain information about exchange rate movements. Over 70% of the variation in Dahlquist and Pénasse (2022)'s missing risk premium can be accounted for by using the entire yield curves, and adding real yield factors explains even more. We interpret these results as support for our approach to model the exchange rate accounting identity based on entire yield curve movements, and they point toward the close link between FX and bond market movements.

Next, in Table 3 we address the comovement between the real exchange rate and its components for yield differentials of 2- and 10-year maturities. For presentation purposes, we denote country differentials by adding "ˆ", e.g., $E_t\left[\hat{\pi}^m\right] = E_t\left[\pi^{m,*} - \pi^m\right]$. Focusing on the observed real exchange rate (q_t), we find a positive correlation with the bond level factor (0.73), positive correlations with slope and curvature factors (0.90 and 0.63, respectively), a positive association with the level of inflation swap differentials (0.19) and a negative comovement with its slope (-0.16). The correlation between the real exchange rate and the term structure of the interest rate exhibits an inverse U-shaped pattern. The correlation is high at the short end (0.72 at the 3-month maturity); it increases slightly to 0.89 at the 2-year maturity and then reverts back to 0.64 at the 10-year maturity (see Chart 3).

We further dissect the correlation pattern by disentangling the interest rate differential into the expected future short rate differential and the term premium differential. Chart 4 depicts an interesting finding: the correlation between the real exchange rate and the term structure of the expectation component is very high and relatively stable along the maturity line. That correlation is higher than the correlation between the exchange rate and the interest rate differential. This is a result of a negative correlation between the exchange rate and the term premium differential for most maturities, which means that an increase in the risk premium requires market participants to invest in a long-term Canadian obligation (relative to that of the United States) and results in a depreciation of the Canadian dollar.

We turn our attention to the FX risk premium. The correlation between the exchange rate and the FX risk premium is very high and negative (see Chart 4) regardless of the horizon, implying that this premium is probably the main component driving the variation in the exchange rate (we confirm this using a variance decomposition). This very robust finding is in line with intuition and with the accounting decomposition given in Equation (5). Lastly, we find the correlation of the expected component of the interest rate differential and the FX risk premium is significantly negative, suggesting that a decrease in the expected interest rate differential is accompanied by an increase in the FX risk premium, which ultimately results in a decrease of the real exchange rate.

The comovements between the real exchange rate and its components are far from constant. Based on a 252-day moving window, Chart 1 displays a time-varying correlation coefficient between

the real exchange rate and the interest rate differential. The correlation is positive most of the time but occasionally switches sign and, at times, is highly negative. This has been the case recently as the correlation hovers around -0.8. The underlying reasons for these changes in the correlation are beyond the scope of this paper. But, consistent with our analysis so far, the FX risk premium is at the heart of these changes. We verify that periods with high volatility of the FX risk premium are periods with lower (and recently negative) correlation between the real exchange rate and the interest rate differential (see Chart 5).[6]

Based on a 252-day moving window, Chart 6 displays a time-varying variance-covariance decomposition. To ease interpretation, we divide all the variance and covariance terms by the variance of the real exchange rate, such that the sum of the individual components is 100%. At short-term (2-year) maturities, real exchange rate volatility dynamics are driven largely by the risk premium, as shown by the large red areas. In addition, the covariance terms between all components (beige) are largely positive except at the end of 2020 and during the onset of the COVID-19 pandemic. In contrast, when considering yield differentials with a 10-year maturity, we find the direct impact of the FX risk premium is comparably smaller, while the sum of the covariance terms plays a larger role. These terms are not only bigger in magnitude but also more frequently show a negative sign.

To complement the previous results, lastly in Table 4, we present the summary statistics of the real exchange rate and its components. As shown, the persistence of the real exchange rate as measured by its half-life, $H(\rho)$, is largely driven by the slow-moving FX risk premium component. In contrast, the mean reversions of the yield differential and term premium are much faster. This is further evidence for the different adjustment speeds between FX and bond markets.

5.2 Time series dynamics

The real exchange rate decomposition allows us to depict the time series dynamics of the individual components. It also provides insights into whether specific factors play a particular important role at certain points in time for the directional moves of the exchange rate. In Chart 7 we document the level of the log exchange rate (black line) and the factor contributions of the individual components.

[6] In untabulated regressions, we confirm that an increase in the volatility of the FX risk premium is associated with a significant decline in the correlation between the real exchange rate and the interest rate differential.

We focus on interest rates with a maturity of 2 years (top graph) and 10 years (bottom graph), due to the policy relevance of these instruments. In addition, in Chart 8 we show the cumulative first difference of the log real exchange rate and the factor contributions since the beginning of 2020. Highlighting this period provides additional insights into the factor contributions during the COVID-19 pandemic.

First, focusing on the real exchange rate in Chart 7, we note the FX risk premium is largely positive between 2008 and 2015 and appears to decline thereafter for the decomposition based on bonds with 2-year investment horizons. For longer maturities, the FX premium is large in magnitude and remains positive throughout the entire sample period. Second, bond-market-based components contribute a comparatively small fraction to the overall price dynamics, which might be expected considering the low interest rate environment since the global financial crisis. Lastly, the expected inflation differential enters the decomposition negatively for both maturities, and it appears to grow slightly in the last few months of our sample.

Next, focusing on the start of the COVID-19 crisis, the chart documents a strong decline in the cumulative change of log real returns (black line) in mid-March. These currency movements imply an appreciation of the US dollar vis-à-vis the Canadian dollar, likely driven by flight-to-safety pressures in the high-uncertainty environment during the early days of the pandemic. Interestingly, the drop in the value of the exchange rate is largely driven by an increase in the FX risk premium, while the contribution of yields and term risk premia are comparably small for short-horizon bonds. In the months following March 2020, the Canadian dollar regained most of its value and even exceeded its pre-crisis level toward the end of our sample period. Lastly, comparing the different tenures, we note that the term premium component has been growing in recent months and, as expected, has a larger impact for the decomposition based on bonds with 10 years' maturity than for bonds with a 2-year investment horizon.

5.3 The risk premium channel

In the previous section, we outline descriptive characteristics of the individual exchange rate components and summarize how they evolve over time. In this section, we take an event study approach and analyze the channels through which monetary policy decisions and macroeconomic news announcements are incorporated into the exchange rate. As the decomposition can be calculated at

a daily frequency, we can pin down the exact reaction of every individual component on announcement days and quantify their importance for daily exchange rate movements.

We start the analysis by examining how information from the Bank of Canada's monetary policy announcements are incorporated into the exchange rate. To this end, we regress the daily change in the real exchange rate (and its components) on level and slope shocks constructed from intraday futures price quotes:

$$\Delta y_t = c + \beta_1 LEV_t + \beta_2 SLP_t + \varepsilon_t,$$

where Δy_t is the change of the real exchange rate, or the expected appreciation, or each of the exchange rate components, i.e., $y_t = E\left[q_{t+m}\right] - q_t$, q_t, $E\left[q_{t+m}\right]$, $\hat{\pi}$, $\hat{i}$, $\hat{y}$, $\hat{TP}$ or $E_t[r_t]$. The level factor (LEV_t) is defined as the change in the median price of BAX futures contracts with a maturity of 1 or 3 months in a short window around the announcement, such as

$$LEV_t = \overline{BAX}^{3,1}_{t,[h+20:h+10]} - \overline{BAX}^{3,1}_{t,[h-15:h-25]},$$

where $\overline{BAX}^{3,1}_{t,[h+20:h+10]}$ refers to the median short-term (1-/3-month) BAX futures rate from 10 to 20 minutes after the announcement time h on day t, and $\overline{BAX}^{3,1}_{t,[h-15:h-25]}$ is the median short-term BAX futures rate from 15 to 25 minutes before the announcement time.

The slope factor is defined as

$$SLP_t = \Delta\overline{BAX}^{15,13}_t - \Delta\overline{BAX}^{3,1}_t,$$

where $\Delta\overline{BAX}^{15,13}_t$ refers to the change in the median long-term (13-/15-month) BAX futures rate and $\Delta\overline{BAX}^{3,1}_t$ is the change in the median short-term (1-/3-month) BAX futures rate in the same narrow window around each monetary policy announcement as used for LEV_t. To avoid the impact of outliers and stale quotes, we use the median price in windows before and after monetary policy announcements, and we consider only those days when the futures contracts are actively traded. Summary statistics for the level and slope components are shown in Panel A of Table 5, while regression results for different maturities are shown in panels B and C.

First, we note that the shock magnitude during the period following the global financial crisis has been relatively small but volatile. For example, the LEV and SLP have an average size of -0.79 basis points (bps) and -0.14 bps and fluctuate by 5.55 bps and 2.90 bps, respectively. As indicated by the distributional characteristics, the range of the shocks varies between -27.25 bps (-8.75 bps) and 11.25 bps (7.00 bps), suggesting that on some announcement days, the yield curve responded substantially around monetary policy announcements.

Regarding the impact of the monetary shocks, we find that a 25 bps increase in LEV results in a 1.75% appreciation of the CAD real exchange rate on the day of the monetary policy announcement. We note that this impact is considerable as the average magnitude of LEV during our sample is only -0.79 bps. Further, since we use daily changes of the real exchange rate as the left-hand side variable–i.e., the change in the currency value is not measured in a small time window around the announcement, but over the day–the regression coefficient might also capture the impact of other developments happening on monetary policy days. This is important to keep in mind given that our sample includes volatile periods, including the months of the global financial crisis and the onset of the COVID-19 pandemic. With this in mind, we find that the communication of the future interest rate path (SLP) also has a large impact, moving the real exchange rate by more than 2%. Further, an immediate increase in the value of the CAD vis-à-vis the USD is associated with an expected depreciation, as shown in the first column. In terms of magnitude, this expected depreciation is largely driven by the immediate appreciation of the CAD on the day of the monetary policy announcement, while the economic effect of $\Delta E_t\left[q_{t+m}\right]$ is comparably small.

Next, focusing on the other exchange rate components, we find that a large proportion of the movements in the exchange rate is driven through the FX risk premium, pointing toward a risk premium channel of monetary policy. More than 80% of the exchange rate changes on monetary policy announcement days can be attributed to the FX risk premium, while changes of bond market factors are smaller and often not significant for the slope factor. These findings are further confirmed in Panel C, though the roles of the yield differential and term premia become more prevalent for long-term maturity bonds. Yet, the FX risk premium continues to be the largest single force for currency dynamics.

To further assess the impact of monetary policy shocks across bond maturities on some of the

exchange rate components, Table 6 documents the changes of the FX risk premium (Panel A) and the expected inflation differential (Panel B). Focusing on Panel A, we find that the impact of a 25 bps LEV (SLP) shock ranges between -0.2% (-0.2%) and 2.0% (3.4%), whereby the significance levels progressively increase with the length of the bond maturities. The table suggests that interest rate adjustments affecting the short end of the curve have comparably less impact on the risk premium, but the effects are amplified for changes of long-term maturities. Similar dynamics can be found for the inflation differential, though both shocks become strongly significant only for maturities of 5 years or longer.

While the event analysis so far has focused on monetary policy announcement days, in a last step we consider all macroeconomic news announcements. To this end, we follow the approach in Altavilla, Giannone and Modugno (2017) and assess whether macroeconomic news surprises explain the variation in exchange rates at different frequencies. Following the methodology in Altavilla, Giannone and Modugno (2017), we measure the change of the real exchange rate (and its components) to macroeconomic news as

$$\Delta y_t^\tau = c + \sum_{i=1}^{n} \beta_i^\tau news_{i,t} + \epsilon_t^\tau,$$

where Δy_t^τ denotes the daily change of the real exchange rate or its components with interest rates of maturity τ. The regressor $news_{i,t}$ is the surprise news component of macroeconomic data announcements, defined as the difference between the published data and the median forecast. If no announcement of variable i takes place on day t, then $news_{i,t} = 0$.

Next, we construct a daily news index as $nix_t^{1,\tau} := \widehat{\Delta^D y_t^\tau}$ based on the fitted values from the aforementioned regression at the daily frequency (as indicated by the superscript D). We also aggregate the fitted values as well as the changes in real exchange rates and individual components to the monthly and quarterly frequency ($f = M, Q$), such that

$$\Delta^f y_t^\tau := y_t^\tau - y_t - f^\tau = \sum_{j=0}^{f-1} \Delta y_{t-j}^\tau$$

and

$$nix_t^{f,\tau} = \sum_{j=0}^{f-1} nix_{t-j}^{D,\tau}.$$

This allows us to assess the explanatory power of macroeconomic news at different frequencies. To be precise, we estimate the regression model

$$\Delta^f y_t^\tau = \gamma^{f,\tau} nix^{f,\tau} + \nu_t^{f,\tau},$$

where the regression coefficient $\gamma^{f,\tau}$ measures the impact of the aggregated news surprises on the real exchange rate or it components.

In Table 7 we summarize the results for news surprises in Canada, focusing on bonds with maturities of 2 years and 10 years, as well as the response of the (expected) appreciation, expected inflation and the FX risk premium at the monthly (Panel A) and quarterly (Panel B) frequency. We document several take-aways. First, the explanatory power of local news surprises increases with the length of the sampling frequency. While the adjusted R^2 reaches a maximum value of 3.52% across columns at the monthly frequency, it increases up to 12.82% at the quarterly frequency. Second, at the monthly frequency, news surprises affect the real exchange rate through the FX risk premium at primarily long investment horizons. In contrast, we find that the impact of the FX risk premium is also significant for shorter maturities at the quarterly frequency. For example, a one-standard-deviation increase of news surprises in Canada leads to an increase of the FX risk premium of at least 1.01 bps. Overall, the table suggests that the risk premium channel also plays an important role for macroeconomic news announcements.

Lastly, in Table 8, we repeat the analysis but consider news surprises from Canadian and US macroeconomic data announcements. We augment the previous equation and estimate the regression

$$\Delta^f y_t^\tau = \delta_{CA}^{f,\tau} nix_{CA}^{f,\tau} + \delta_{US}^{f,\tau} nix_{US}^{f,\tau} + \mu_t^{f,\tau},$$

where the regression coefficients $\delta_{CA}^{f,\tau}$ and $\delta_{US}^{f,\tau}$ measure the impact of the aggregated Canadian and

US news surprises on the real exchange rate, and its components, at the monthly or quarterly frequency ($f = M, Q$), respectively. The results suggest that both foreign and domestic news surprises affect real exchange rate changes through the risk premium channel. At the monthly frequency, news surprises in the United States have a significant impact at the short end of the curve (0.48 bps), while Canadian news surprises are only significant for bonds with long maturities (1.24 bps). Also, the adjusted goodness-of-fit measure increases compared with the measure in Table 7, despite the inclusion of an additional regressor to the model. At the quarterly frequency, the relative importance of news surprises changes in that local news appears to become more important, while the impact of US announcement surprises decays for long-term maturities. This is different for inflation expectations. For both sampling frequencies, US news appears to play a significant role. Overall, the results suggest that domestic and foreign news surprises might have an asymmetric impact on the real exchange rate, and the level of significance varies with the investment horizon.

6 Conclusion

We provide a new real exchange rate decomposition model that combines information on the exchange rate and the cross-section of real and nominal interest rate differentials in the context of a VAR model. The decomposition provides insights into the disconnect, and at times counterintuitive interactions, between the interest rate differential and the exchange rate by quantifying the exact role of individual components. Distinguishing between different factors, we document the dynamics of the real exchange rate and its components in the period following the global financial crisis and show a significant role of an FX risk premium that is largely unrelated to bond market dynamics. Further, we evaluate the impact of macroeconomic news and monetary policy announcements on the exchange rate. We find that both the changes in the expected future spot rate and risk premium are strongly affected by unexpected changes to the Bank of Canada's monetary policy regime, but we identify the foreign exchange risk premium is the main channel through which central bank communications and announcements affect the dynamics of the real exchange rate.

7 Appendix

Table A: Real exchange rate decomposition summary

Variables	Factors $(\bar{X}_t, \eta_t)$	Coefficients
q_t	$\mu_q + \beta_{qx}' \left(\bar{X}_t - \mu_X\right) + \beta_{q\eta}\eta_t$	$\begin{cases} \beta_{qx}' = \left(\bar{b}_1 - \bar{c}_1 - \bar{\beta}\right)' \tilde{\Phi}_\infty \\ \beta_{q\eta} = \left(\bar{b}_1 - \bar{c}_1 - \bar{\beta}\right)' \tilde{\gamma}_\infty - \tilde{\lambda}_\eta^{(\infty)} \end{cases}$
$E_t\left[q_{t+m}\right]$	$\mu_q + \beta_{qx}'\Phi^m \left(\bar{X}_t - \mu_X\right) + \beta_{q\eta}^{(m)}\eta_t$	$\beta_{q\eta}^{(m)} \equiv \beta_{qx}' \left(\lambda_\eta I - \Phi\right)^{-1} \times \left(\lambda_\eta^m I - \Phi^m\right)\gamma + \beta_{q\eta}\lambda_\eta^m$
$(1/m)\sum_{j=1}^m E_t\left[r_{t+j}\right]$	$\alpha + \bar{\beta}'\mu_X + \beta_{rpx}^{(m)\prime}\left(\bar{X}_t - \mu_X\right) + \beta_{rp\eta}^{(m)}\eta_t$	$\beta_{rpx}^{(m)\prime} \equiv \frac{\bar{\beta}'\tilde{\Phi}_m}{m}; \quad \beta_{rp\eta}^{(m)} \equiv \frac{\bar{\beta}'\tilde{\gamma}_m + \tilde{\lambda}_\eta^{(m)}}{m}$
$tp_t^{(m,*)} - tp_t^{(m)}$	$\left(\bar{b}_m - \bar{b}_1\right)'\mu_X + \beta_{tpx}^{(m)\prime}\left(\bar{X}_t - \mu_X\right) + \beta_{tp\eta}^{(m)}\eta_t$	$\beta_{tpx}^{(m)\prime} \equiv \bar{b}_m' - \frac{\bar{b}_1'\tilde{\Phi}_m}{m}; \quad \beta_{tp\eta}^{(m)} \equiv -\frac{\bar{b}_1'\tilde{\gamma}_m}{m}$
$(1/m)\sum_{j=1}^m E_t\left[\pi_{t+j}^* - \pi_{t+j}\right]$	$\mu_\pi^P + \frac{\bar{c}_1'\tilde{\Phi}_m}{m}\left(\bar{X}_t - \mu_X\right) + \frac{\bar{c}_1'\tilde{\gamma}_m}{m}\eta_t$	$\mu_\pi^P = \left(\bar{b}_1 - \bar{\beta}\right)'\mu_X - \alpha$
$(1/m)\sum_{j=0}^{m-1} E_t\left[i_{t+j}^* - i_{t+j}\right]$	$\bar{b}_1'\mu_X + \frac{\bar{b}_1'\tilde{\Phi}_m}{m}\left(\bar{X}_t - \mu_X\right) + \frac{\bar{b}_1'\tilde{\gamma}_m}{m}\eta_t$	
$y_t^{(m*)} - y_t^{(m)}$	$\bar{b}_m'\bar{X}_t$	
$ISR_t^{(m,*)} - ISR_t^{(m)}$	$\bar{c}_m'\bar{X}_t$	
$IRP_t^{(m,*)} - IRP_t^{(m)}$	$\mu_\pi^{rp} + \beta_{ipx}^{(m)\prime}\left(\bar{X}_t - \mu_X\right) - \frac{\bar{c}_1'\tilde{\gamma}_m}{m}\eta_t$	$\mu_\pi^{rp} = \bar{c}_m'\mu_X - \mu_\pi^P;\ \beta_{ipx}^{(m)\prime} = \bar{c}_m' - \frac{\bar{c}_1'\tilde{\Phi}_m}{m}$

Table B: Summary of innovations

Variables	Innovations	Coefficients
q_t	$\rho_{q\eta}\hat{u}^\eta + \beta_{qx}'\Sigma\hat{u}^x$	$\rho_{q\eta} = \beta_{q\eta}\sigma_\eta + \beta_{qx}'\rho_{x\eta}$
$E_t\left[q_{t+m}\right]$	$\rho_{q\eta}^{(m)}\hat{u}^\eta + \beta_{qx}'\Phi^m\Sigma\hat{u}^x$	$\rho_{q\eta}^{(m)} = \beta_{qx}'\Phi^m\rho_{x\eta} + \beta_{q\eta}^{(m)}\sigma_\eta$
$(1/m)\sum_{j=1}^m E_t\left[r_{t+j}\right]$	$\rho_{rp\eta}^{(m)}\hat{u}^\eta + \beta_{rpx}^{(m)\prime}\Sigma\hat{u}^x$	$\rho_{rp\eta}^{(m)} = \beta_{rp\eta}^{(m)}\sigma_\eta + \beta_{rpx}^{(m)\prime}\rho_{x\eta}$
$tp_t^{(m,*)} - tp_t^{(m)}$	$\rho_{tp\eta}^{(m)}\hat{u}^\eta + \beta_{tpx}^{(m)\prime}\Sigma\hat{u}^x$	$\rho_{tp\eta}^{(m)} = \beta_{tp\eta}^{(m)}\sigma_\eta + \beta_{tpx}^{(m)\prime}\rho_{x\eta}$
$(1/m)\sum_{j=1}^m E_t\left[\pi_{t+j}^* - \pi_{t+j}\right]$	$\rho_{\pi\eta}^{(m)}\hat{u}^\eta + \frac{\bar{c}_1'\tilde{\Phi}_m}{m}\Sigma\hat{u}^x$	$\rho_{\pi\eta}^{(m)} = \frac{\bar{c}_1'}{m}\left(\tilde{\Phi}_m\rho_{x\eta} + \sigma_\eta\tilde{\gamma}_m\right)$
$(1/m)\sum_{j=0}^{m-1} E_t\left[i_{t+j}^* - i_{t+j}\right]$	$\rho_{i\eta}^{(m)}\hat{u}^\eta + \frac{\bar{b}_1'\tilde{\Phi}_m}{m}\Sigma\hat{u}^x$	$\rho_{i\eta}^{(m)} = \frac{\bar{b}_1'}{m}\left(\tilde{\Phi}_m\rho_{x\eta} + \sigma_\eta\tilde{\gamma}_m\right)$
$y_t^{(m*)} - y_t^{(m)}$	$\bar{b}_m'\rho_{x\eta}\hat{u}^\eta + \bar{b}_m'\Sigma\hat{u}^x$	
$ISR_t^{(m,*)} - ISR_t^{(m)}$	$\bar{c}_m'\rho_{x\eta}\hat{u}^\eta + \bar{c}_m'\Sigma\hat{u}^x$	
$IRP_t^{(m,*)} - IRP_t^{(m)}$	$\rho_{ip\eta}^{(m)}\hat{u}^\eta + \beta_{ipx}^{(m)\prime}\Sigma\hat{u}^x$	$\rho_{ip\eta}^{(m)} = \beta_{ipx}^{(m)\prime}\rho_{x\eta} - \sigma_\eta\frac{\bar{c}_1'\tilde{\gamma}_m}{m}$

7.1 Estimation

7.1.1 The cross-section of $y_t^{(m*)} - y_t^{(m)}$

The goal is to estimate the yield curve factors X_t, and the loadings b'_m, given in equations (8) and (9). Let us denote $dy_t^{(m)} \equiv y_t^{(m*)} - y_t^{(m)}$ and assume that at each day t, we observe a cross-section of J spread. When we stack them in

$$SY = \left(dy_t^{(m_1)}, dy_t^{(m_2)}, \cdots, dy_t^{(m_J)}\right)',$$

we have

$$SY_t = \begin{pmatrix} b'_{m_1} \\ b'_{m_1} \\ \vdots \\ b'_{m_J} \end{pmatrix} X_t.$$

We assume that three portfolios (characterized by a $3 \times J$ matrix W) of observed spreads match exactly their model counterparts; concretely, this means that

$$SP_t \equiv W \times SY_t = BX_t,$$

where

$$B \equiv W \begin{bmatrix} b_{m_1} & b_{m_1} & \cdots & b_{m_J} \end{bmatrix}',$$

and hence

$$X_t = B^{-1} \times SP_t.$$

Let us denote

$$\varepsilon_{sy,t} \equiv SY_t - \begin{bmatrix} b_{m_1} & b_{m_1} & \cdots & b_{m_J} \end{bmatrix}' B^{-1} \times SP_t.$$

To estimate λ, we minimize

$$\frac{1}{T} \sum_{t=1}^{T} \varepsilon'_{sy,t} \overline{W}' \overline{W} \varepsilon_{sy,t},$$

where $\overline{W}$ is the other portfolios ($(J-3) \times J$) that are measured with error, and $\overline{W}$ is defined such that $\left(\frac{W}{\overline{W}}\right)$ is of rank J. At the end of this first step, we have both X_t and λ; hence we have b'_m for any given maturity m.

7.1.2 *The cross-section of* $ISR_t^{(m,*)} - ISR_t^{(m)}$

We now discuss the estimation of the cross-section of inflation swap spreads. Concretely, the goal is to estimate c'_m, w'_m and the factor Z_t, which appear in Equation (10). To do so, we proceed in three steps:

1. We estimate c_m as the regression coefficient of the observed $ISR_t^{(m,*)} - ISR_t^{(m)}$ on X_t, which is estimated in section (7.1.1).

2. Assuming that Z_t has two elements, we estimate Z_t as

$$Z_t = \begin{pmatrix} (1/J_{isr}) \sum_{j=1}^{J_{isr}} u_t^{(m_j)} \\ u_t^{(30yr)} - u_t^{(10yr)} \end{pmatrix},$$

   where $u_t^{(m)}$ is the regression's residual from step 1.

3. Finally, we estimate w_m as the regression coefficient of $u_t^{(m)}$ on Z_t.

7.1.3 *Parameters for* $E_t\left[r_{t+1}\right]$ *and* $E_t\left[\bar{X}_{t+1}\right]$

We now turn to the estimation of α, $\bar{\beta}$, K_0 and Φ, which appear in the risk premium, yield and inflation spread dynamic given in equations (11) and (12). We estimate α and $\bar{\beta}$, respectively, as the constant and slope of the regression of r_{t+1} on $\bar{X}_t$. Similarly, we estimate K_0 and Φ, respectively, as the constant and slope of the regression of $\bar{X}_{t+1}$ on $\bar{X}_t$. Hence, the estimation of μ_X is $\mu_X = (I - \Phi)^{-1} K_0$. We fix μ_q to the sample average of q_t, that is, $\mu_q = (1/T) \sum_{t=1}^{T} q_t$.

7.1.4 *Estimation of* λ_η *and* γ *as a function of* $\bar{c}_1$

We use equations (13) and (23)to estimate λ_η as a function of $\bar{c}_1$, as follows:

$$\lambda_\eta = \frac{\sum_{t=1}^{T-1} \left(q_t - \mu_q - \beta'_{qx}\left(\bar{X}_t - \mu_X\right)\right)\left(q_{t+1} - \mu_q - \beta'_{qx}\left(\bar{X}_{t+1} - \mu_X\right)\right)}{\sum_{t=1}^{T-1} \left(q_t - \mu_q - \beta'_{qx}\left(\bar{X}_t - \mu_X\right)\right)^2}, \tag{24}$$

where $\beta'_{qx} = \left(\bar{b}_1 - \bar{\beta} - \bar{c}_1\right)' (I - \Phi)^{-1}$. We now turn to the estimation of γ as a function of $\bar{c}_1$. Equation (12) implies that

$$E_t\left[\epsilon_{t+1}\right] = \eta_t \gamma,$$

where $\epsilon_{t+1} \equiv \bar{X}_{t+1} - K_0 - \Phi \bar{X}_t$. Hence, we estimate γ as

$$\gamma = \beta_{q\eta} \bar{\gamma},$$

where $\bar{\gamma}$ is given by:

$$\bar{\gamma} \equiv \frac{\sum_{t=1}^{T-1}\left(q_t - \mu_q - \beta_{qx}'\left(\bar{X}_t - \mu_X\right)\right)\epsilon_{t+1}}{\sum_{t=1}^{T-1}\left(q_t - \mu_q - \beta_{qx}'\left(\bar{X}_t - \mu_X\right)\right)^2}.$$

Recall that

$$\begin{aligned}
\beta_{q\eta} &= \left(\bar{b}_1 - \bar{\beta} - \bar{c}_1\right)'\left(\frac{1}{1-\lambda_\eta}I - (I-\Phi)^{-1}\right)(\lambda_\eta I - \Phi)^{-1}\gamma - \frac{1}{1-\lambda_\eta} \\
&= \beta_{q\eta}\left(\bar{b}_1 - \bar{\beta} - \bar{c}_1\right)'\left(\frac{1}{1-\lambda_\eta}I - (I-\Phi)^{-1}\right)(\lambda_\eta I - \Phi)^{-1}\bar{\gamma} - \frac{1}{1-\lambda_\eta},
\end{aligned}$$

and hence, we have

$$\beta_{q\eta} = -\frac{1}{1-\lambda_\eta}\frac{1}{1-\delta},$$

where

$$\delta \equiv \left(\bar{b}_1 - \bar{\beta} - \bar{c}_1\right)'\left(\frac{1}{1-\lambda_\eta}I - (I-\Phi)^{-1}\right)(\lambda_\eta I - \Phi)^{-1}\bar{\gamma}.$$

7.1.5 Estimation of $\bar{c}_1$

Recall that

$$\begin{aligned}
& (1/m)\sum_{j=1}^{m} E_t\left[\pi_{t+j}^* - \pi_{t+j}\right] \\
= \;& \mu_\pi + \bar{c}_1'(1/m)\sum_{j=0}^{m-1} E_t\left[\bar{X}_{t+j}\right] \\
= \;& \left(\bar{b}_1 - \bar{c}_1 - \bar{\beta}\right)'\mu_X - \alpha + \bar{c}_1'(1/m)\sum_{j=0}^{m-1} E_t\left[\bar{X}_{t+j}\right] \\
= \;& \left(\bar{b}_1 - \bar{c}_1 - \bar{\beta}\right)'\mu_X - \alpha + \bar{c}_1'\left(\mu_X + \frac{\tilde{\Phi}_m}{m}\left(\bar{X}_t - \mu_X\right) + \frac{\tilde{\gamma}_m}{m}\eta_t\right) \\
= \;& \left(\bar{b}_1 - \bar{\beta}\right)'\mu_X - \alpha + \bar{c}_1'\left(\frac{\tilde{\Phi}_m}{m}\left(\bar{X}_t - \mu_X\right) + \frac{\tilde{\gamma}_m}{m}\eta_t\right).
\end{aligned}$$

We use the monthly observation for $(1/m)\sum_{j=1}^{m} E_t\left[\pi_{t+j}^* - \pi_{t+j}\right]$ at several horizons, for instance from the Survey of Professional Forecasters (SPF). We can estimate $\bar{c}_1$ by minimizing

$$\sum_{t=1}^{T}\sum_{m\in\{m_1,\cdots,m_J\}}\left(\varepsilon_t^{(m)}\right)^2,$$

where

$$\varepsilon_t^{(m)} \equiv dSPF_t^{(m)} - \left[\left(\bar{b}_1 - \bar{\beta}\right)'\mu_X - \alpha + \bar{c}_1'\left(\frac{\tilde{\Phi}_m}{m}\left(\bar{X}_t - \mu_X\right) + \frac{\tilde{\gamma}_m}{m}\eta_t\right)\right]$$

with $dSPF_t^{(m)}$, the survey equivalent of $(1/m)\sum_{j=1}^{m} E_t\left[\pi^*_{t+j} - \pi_{t+j}\right]$.

7.1.6 Estimation of Σ, $\rho_{x\eta}$ and σ_η

To estimate σ_η, compute the time series of $\bar{u}^\eta_{t+1} \equiv \eta_{t+1} - \lambda_\eta \eta_t$, then

$$\sigma_\eta = \sqrt{\frac{\sum_{t=2}^{T}\left(\bar{u}^\eta_{t+1}\right)^2}{T-1}}.$$

Given that we have already estimated σ_η, we can compute the time series of u^η_{t+1} as $u^\eta_{t+1} = \frac{\bar{u}^\eta_{t+1}}{\sigma_\eta}$. To estimate $\rho_{x\eta}$, we compute the time series of $\bar{u}^x_{t+1} = \bar{X}_{t+1} - \mu_X - \left[\Phi\left(\bar{X}_t - \mu_X\right) + \gamma\eta_t\right]$; then we regress each component (there are five) of $\bar{u}^x_{t+1}$ on u^η_{t+1}. Each coefficient of these five regressions gives us the five components of $\rho_{x\eta}$. Since we have $\rho_{x\eta}$, we can compute the following time series:

$$\tilde{u}^x_{t+1} = \bar{u}^x_{t+1} - \rho_{x\eta} u^\eta_{t+1},$$

then compute the following:

$$\Omega_x = \frac{\sum_{t=2}^{T}\tilde{u}^x_{t+1}\left(\tilde{u}^x_{t+1}\right)^T}{T-1}$$

and take the lower triangular Cholesky decomposition of Ω_x to get Σ.

7.2 Benchmark models

7.2.1 No information from the inflation swap curve

$$\bar{\beta} = \begin{pmatrix} \beta \\ \varphi \end{pmatrix} = \begin{pmatrix} \beta \\ 0 \end{pmatrix}; \quad \bar{c}_1 = \begin{pmatrix} c_1 \\ w_1 \end{pmatrix} = \begin{pmatrix} 0 \\ 0 \end{pmatrix} = 0;$$

$$\Phi = \begin{bmatrix} \Phi_x & \Psi_{xz} \\ \Psi_{zx} & \Phi_z \end{bmatrix} = \begin{bmatrix} \Phi_x & 0 \\ 0 & \Phi_z \end{bmatrix}; \quad \Sigma = \begin{bmatrix} \Sigma_x & \Sigma_{xz} \\ \Sigma_{zx} & \Sigma_z \end{bmatrix} = \begin{bmatrix} \Sigma_x & 0 \\ 0 & \Sigma_z \end{bmatrix}.$$

7.2.2 No information from nominal yield and inflation swap curves

In addition to the previous constraints, we want to have

$$\beta' X_t = \beta_i\left(y_t^{(1*)} - y_t^{(1)}\right) \tag{25}$$

$$y_t^{(1*)} - y_t^{(1)} = b_1' X_t \sim AR(1), \tag{26}$$

which imply that only the short rate differential $y_t^{(1*)} - y_t^{(1)}$ matters for the exchange rate decomposition. Hence this corresponds to the model proposed in Dahlquist and Pénasse (2022).

Equation (25) is equivalent to

$$\beta' X_t = \beta_i \left(y_t^{(1*)} - y_t^{(1)} \right) = \beta_i b_1' X_t;$$

hence

$$\beta = \beta_i b_1.$$

We estimate β_i as the regression coefficient of r_{t+1} on $y_t^{(1*)} - y_t^{(1)}$, or the shortest maturity $y_t^{(m*)} - y_t^{(m)}$ in the sample.

Turning to Equation (26), we recall that

$$E_t \left[X_{t+1} \right] = K_x + \Phi_x X_t + \eta_t \gamma_x,$$

which implies that

$$E_t \left[b_1' X_{t+1} \right] = b_1' K_x + b_1' \Phi_x X_t + \eta_t b_1' \gamma_x.$$

Hence it must be the case that

$$b_1' \Phi_x = \phi_i b_1' \tag{27}$$

$$b_1' \gamma_x = 0. \tag{28}$$

Equation (27) holds by setting $\gamma_x = 0$. Equation (28) means that b_1 is an eigenvector for Φ_x', which holds if we re-express Φ_x' as follows:

$$\begin{aligned} \Phi_x' &= V \begin{bmatrix} \lambda_l & 0 & 0 \\ 0 & \lambda_s & 0 \\ 0 & 0 & \lambda_c \end{bmatrix} V^{-1} \Longleftrightarrow \Phi_x = (V')^{-1} \begin{bmatrix} \lambda_l & 0 & 0 \\ 0 & \lambda_s & 0 \\ 0 & 0 & \lambda_c \end{bmatrix} V' \\ V &= \begin{bmatrix} b_1 & V_{:2} & V_{:3} \end{bmatrix}, \end{aligned}$$

where

$$V_{:2} = \begin{pmatrix} V_{12} \\ 1 \\ V_{32} \end{pmatrix}, \quad V_{:3} = \begin{pmatrix} V_{13} \\ V_{23} \\ 1 \end{pmatrix}.$$

To estimate K_x and Φ_x, we minimize the sum of squared errors

$$X_{t+1} - (K_x + \Phi_x X_t)\,.$$

The parameters to be estimated are K_0, V_{12}, V_{32}, V_{13}, V_{23}, $\tilde{\lambda}_l$, $\tilde{\lambda}_s$ and $\tilde{\lambda}_c$, where $\tilde{\lambda}_l$, $\tilde{\lambda}_s$ and $\tilde{\lambda}_c$ are such that

$$\lambda_j = \frac{1}{1 + \exp\left(-\tilde{\lambda}_j\right)} \text{ for } j \in \{l, s, c\}\,.$$

Charts

Chart 1: **Time-varying correlation: real exchange rate and yield differentials**

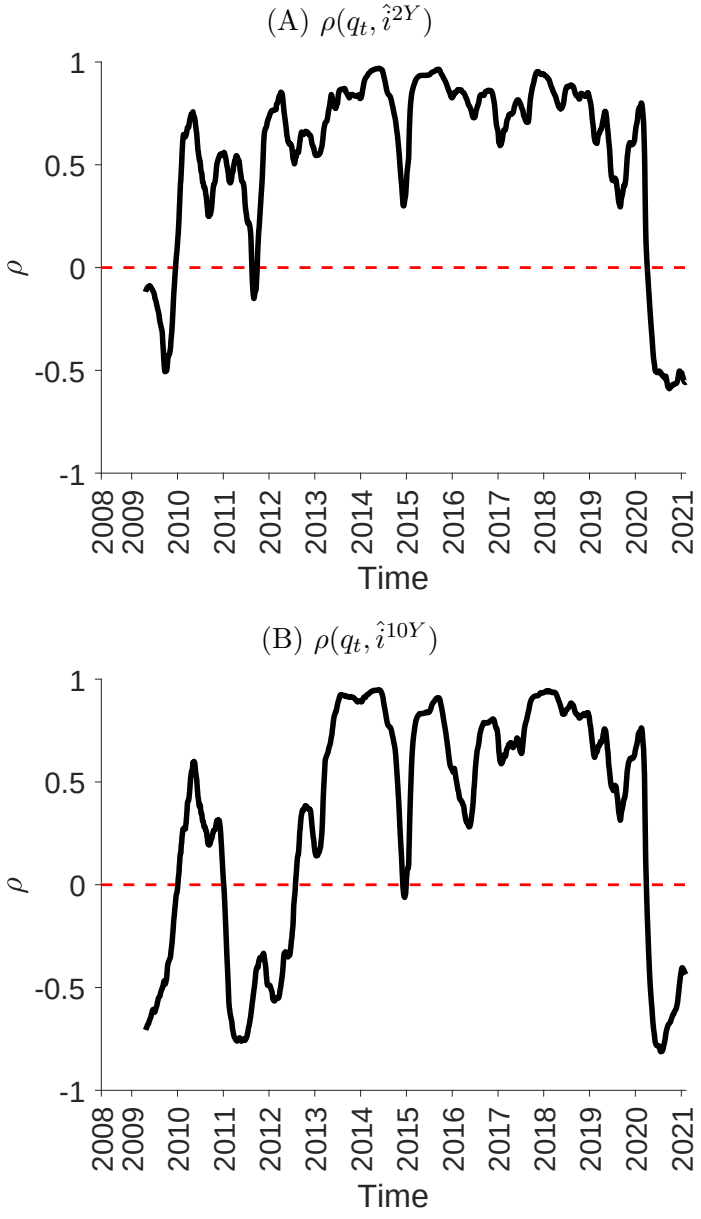

Note: The chart shows time-varying correlation coefficients (ρ), based on a 252-day rolling window, of the real exchange rate (q) and the observed yield differential between Canada and the United States. The top (bottom) graph is based on the yield differential with a maturity of 2 years (10 years). The red dashed line indicates a correlation coefficient of zero. The notation $\hat{x}^m$ denotes the difference in observed yields with maturity m, e.g., $\hat{x} = (x^{m*} - x^m)$. The sample period is from May 8, 2008, to February 5, 2021.

Chart 2: **Time series dynamics: real exchange rate and interest rate differential**

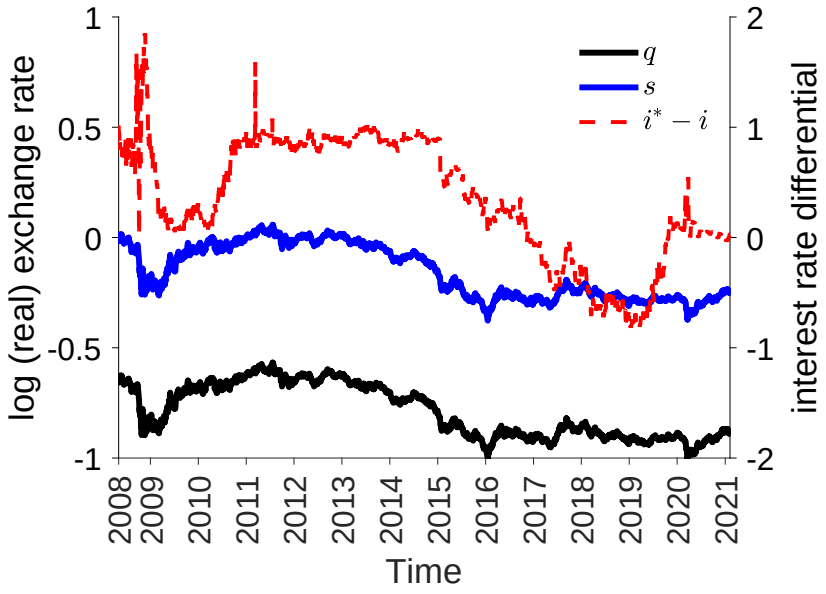

Note: The chart shows the time series dynamics of the log real (q, black) and log nominal (s, blue) exchange rate (left y-axis). The red dashed line presents dynamics of the interest differential (right y-axis) between Canada (i^*) and the United States (i). The sample period is from May 8, 2008, to February 5, 2021.

Chart 3: **Sample correlations for various bond maturities**

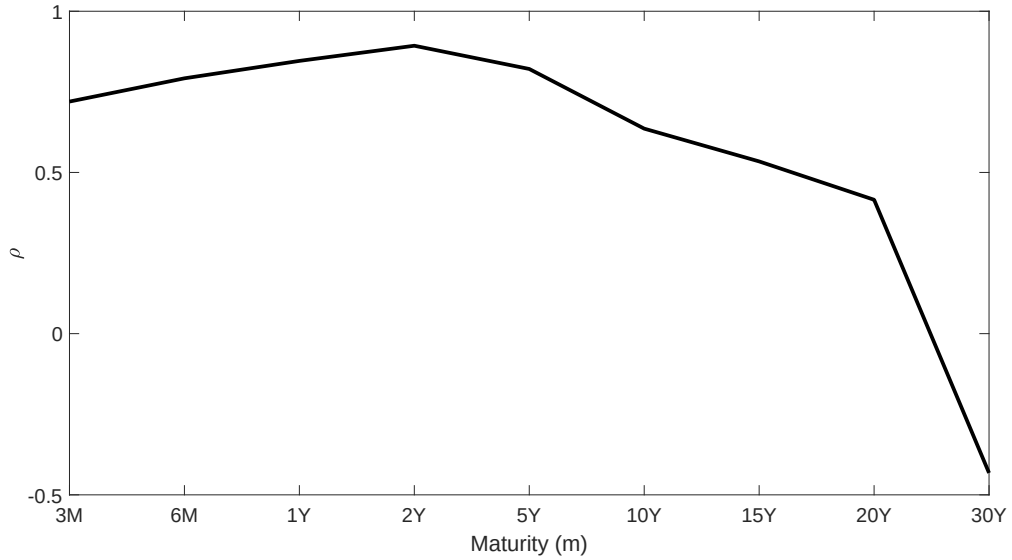

Note: The chart shows the sample correlation coefficients (y-axis) between the real exchange rate and the observed yield differential for different maturities (x-axis). The sample period is from May 8, 2008, to February 5, 2021.

Chart 4: **Sample correlations of exchange rate, expected interest rate differential, and FX premium**

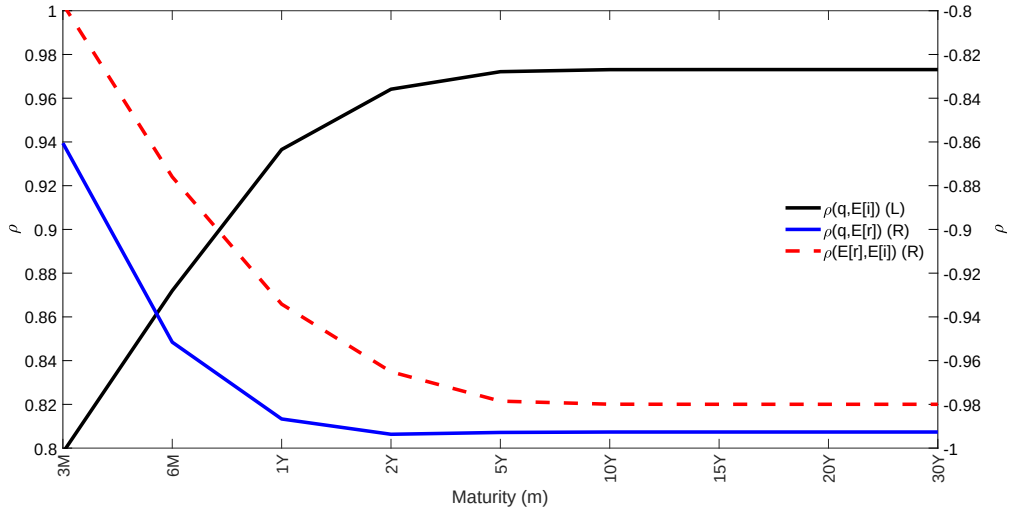

Note: The chart shows the sample correlation coefficients (y-axes) between the real exchange rate and the expected interest rate differential (left axis), the real exchange rate and the FX risk premium (right axis), as well as the expected FX risk premium and the expected interest rate differential (right axis) for different maturities (x-axis). The sample period is from May 8, 2008, to February 5, 2021.

Chart 5: **Sample correlations and the volatility of the FX risk premium**

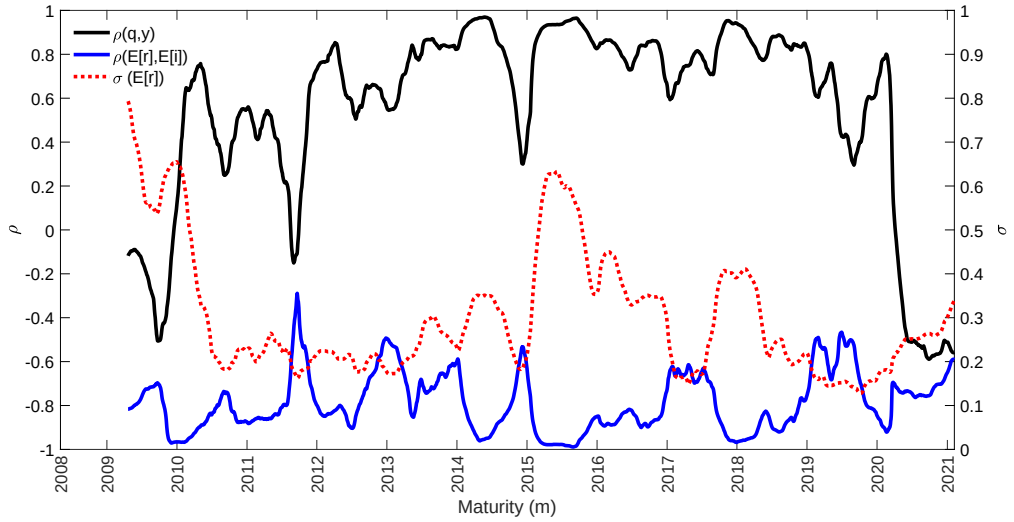

Note: The chart shows time-varying correlation coefficients (ρ), based on a 252-day rolling window, of the real exchange rate (q) and the model-implied yield differential ($\rho(E[r], y)$, left y-axis), the moving correlation coefficient between the FX risk premium and expected short-term differential ($\rho(E[r], E[i])$, left y-axis), and the time-varying volatility of the FX risk premium ($\sigma(E[r])$, right y-axis). The sample period is from May 8, 2008, to February 5, 2021.

Chart 6: **Time-varying variance decomposition: real exchange rate**

(A) **Full sample: 2 years**

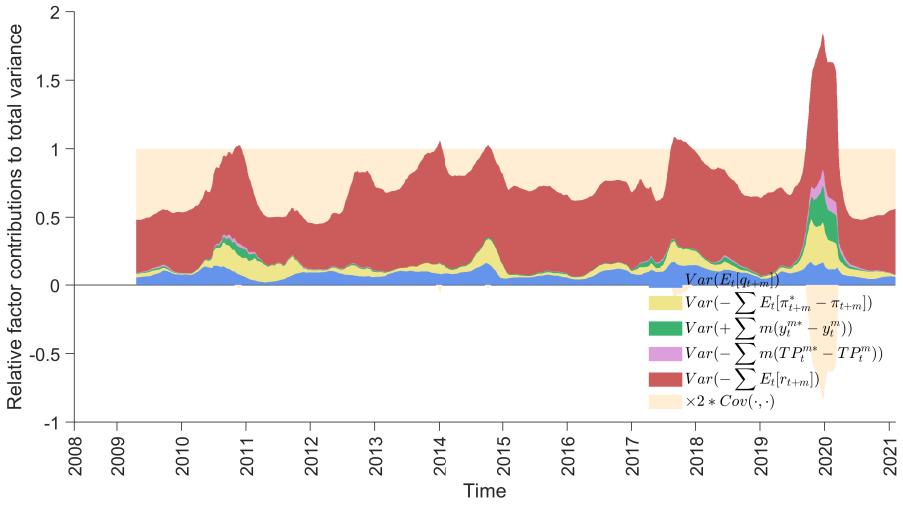

(B) **Full sample: 10 years**

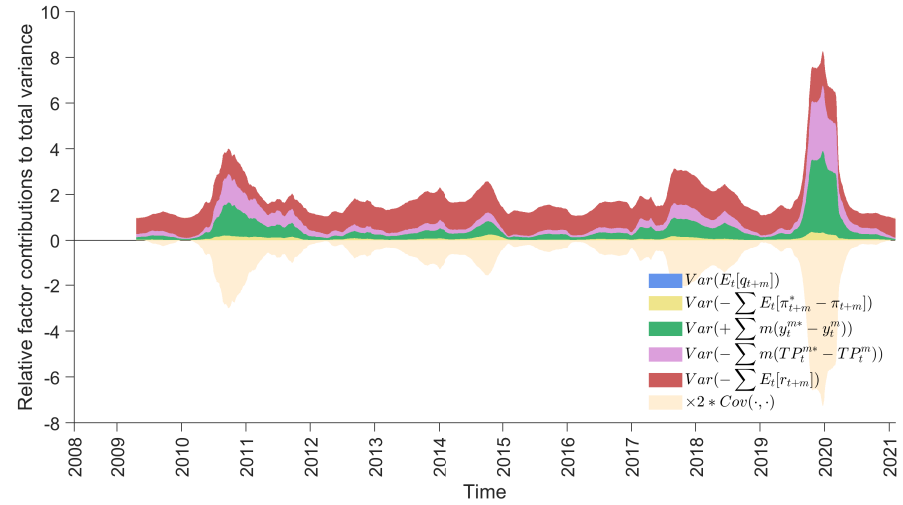

Note: The chart shows a time-varying variance-covariance-decomposition, based on a 252-day rolling window, of the individual components of the following real exchange rate decomposition:

$$q_t = E_t\left[q_{t+m}\right] - \sum_{j=1}^{m} E_t\left[\pi^*_{t+j} - \pi_{t+j}\right] + m\left(y_t^{(m*)} - y_t^{(m)}\right) - m\left(TP_t^{(m*)} - TP_t^{(m)}\right) - \sum_{j=1}^{m} E_t\left[r_{t+j}\right].$$

Covariance terms are aggregated to one component and shown by the light-beige area. All individual components are normalized by the variance of the real exchange rate, such that the individual components sum up to one. The top (bottom) graph is based on yield differentials with 2-year (10-year) maturity. The sample period is from May 8, 2008, to February 5, 2021.

Chart 7: **Real exchange rate decomposition: full sample**

(A) **Full sample: 2 years**

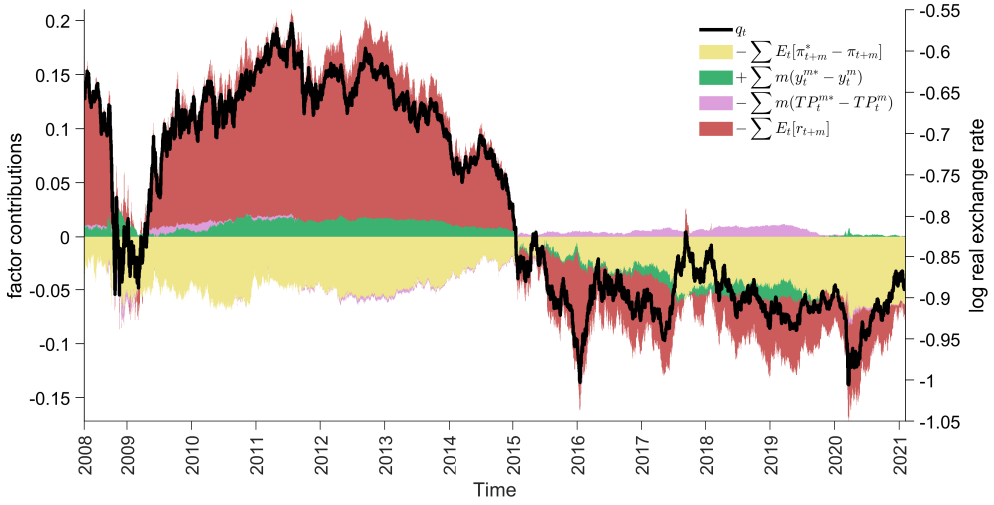

(B) **Full sample: 10 years**

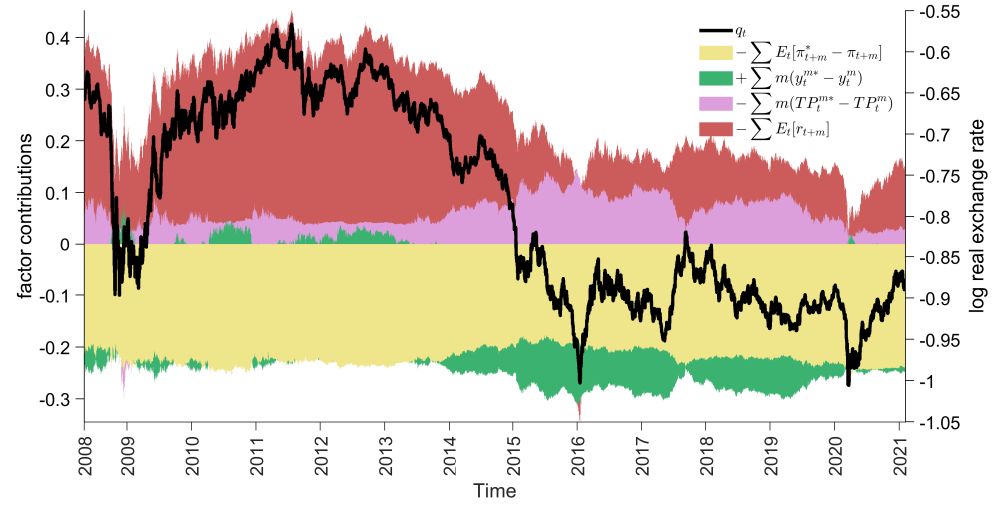

Note: The chart shows time series dynamics of the individual components of the real exchange rate decomposition

$$q_t = E_t\left[q_{t+m}\right] - \sum_{j=1}^{m} E_t\left[\pi^*_{t+j} - \pi_{t+j}\right] + m\left(y_t^{(m*)} - y_t^{(m)}\right) - m\left(TP_t^{(m*)} - TP_t^{(m)}\right) - \sum_{j=1}^{m} E_t\left[r_{t+j}\right],$$

where the factor contributions are depicted on the left y-axis, while dynamics of the real exchange rate (q) are measured on the right y-axis. The top (bottom) graph is based on yield differentials with 2-year (10-year) maturity. The component $E_t\left[q_{t+m}\right]$ is omitted for presentation purposes. The sample period is from May 8, 2008, to February 5, 2021.

Chart 8: **Real log returns decomposition**

(A) **Full sample: 2 years**

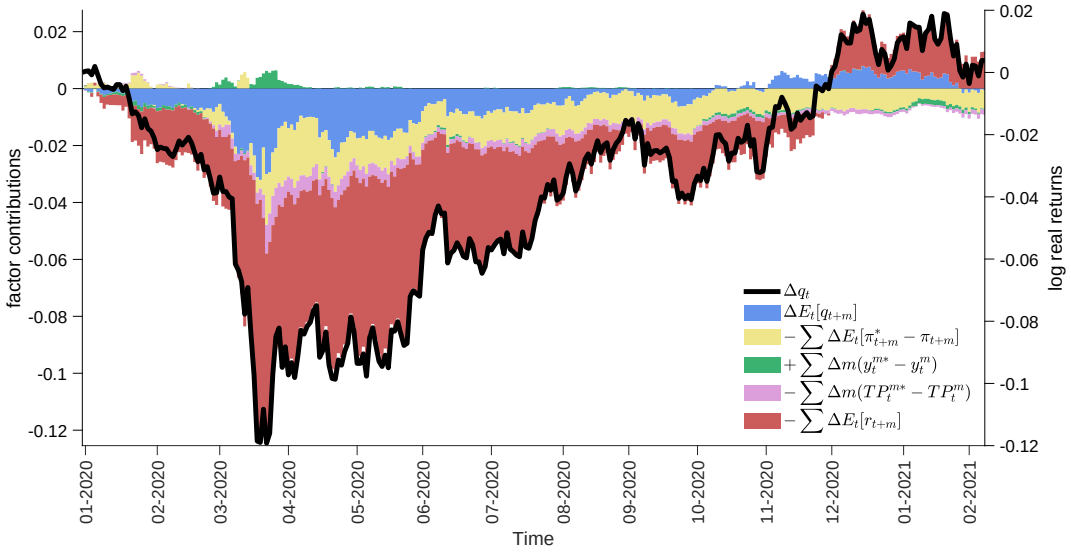

(B) **Full sample: 10 years**

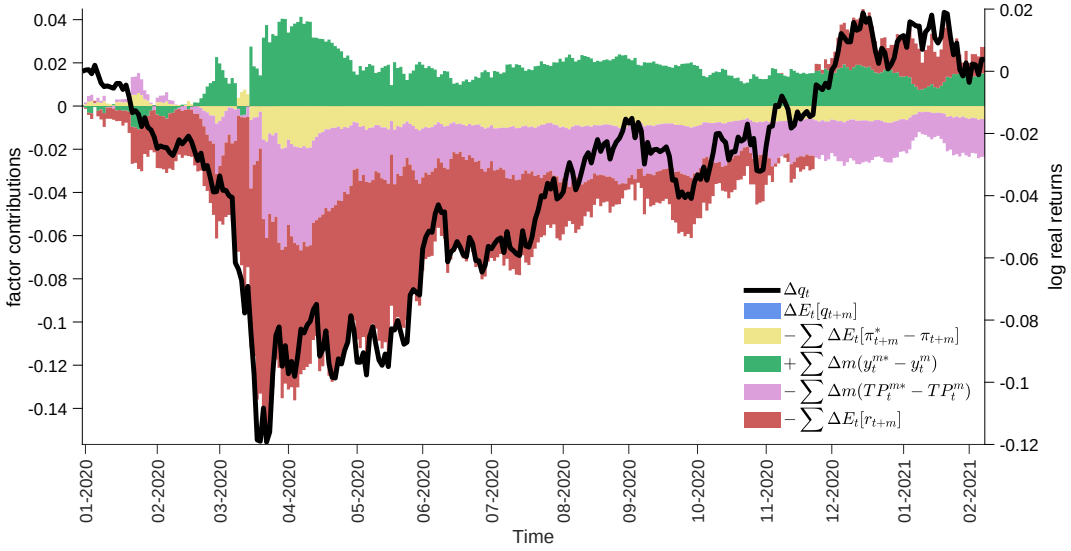

Note: The chart shows time series dynamics of the first difference of the individual components of the real exchange rate decomposition

$$\Delta q_t = \Delta E_t\left[q_{t+m}\right] - \sum_{j=1}^{m} \Delta E_t\left[\pi^*_{t+j} - \pi_{t+j}\right] + \Delta m\left(y_t^{(m*)} - y_t^{(m)}\right) - \Delta m\left(TP_t^{(m*)} - TP_t^{(m)}\right) - \sum_{j=1}^{m} \Delta E_t\left[r_{t+j}\right],$$

where changes in factor contributions are depicted on the left y-axis, while real log returns (Δq) are measured on the right y-axis. The sample period is from January 4, 2020, to February 8, 2021.

Tables

Table 1: **Model fit and benchmark models**

This table reports regression results to the model

$$r_{t+1} - \eta_t \quad = \quad \alpha + \beta' X_t + \varphi' Z_t + \varepsilon_{t+1},$$

where $r_{t+1} - \eta_t$ is the difference between the realized exchange rate excess return in period $t+1$ and the model-implied missing risk premium (η_t), X_t contains nominal yield factors, and Z_t contains factors measuring the cross-section of inflation swaps. In the column BM1 (i.e., benchmark model 1), we impose the restriction $\varphi = 0$. In the column BM2, all coefficients except β_1 are restricted to be zero. Results are presented for data sampled at daily, monthly and quarterly frequencies. Numbers in parentheses refer to t-statistics based on Newey-West standard errors. The sample period is from May 8, 2008, to February 5, 2021.

	Daily			Monthly			Quarterly		
	Full	BM1	BM2	Full	BM1	BM2	Full	BM1	BM2
α	0.00	0.00	0.00	0.00	0.00	0.00	0.00	0.00	0.00
	(-0.21)	(-0.01)	(-0.61)	(0.07)	(0.22)	(-0.24)	(0.10)	(0.22)	(-0.27)
X_1	0.29	2.10		-2.14	-1.13		-0.95	-0.58	
	(0.01)	(0.12)		(-0.22)	(-0.11)		(-0.09)	(-0.06)	
X_2	-1.62	-2.24		-5.15	-4.86		-3.99	-3.77	
	(-0.24)	(-0.34)		(-1.37)	(-1.13)		(-0.75)	(-0.73)	
X_3	4.61	4.83		3.74	3.70		3.80	3.38	
	(1.14)	(1.37)		(2.15)	(2.40)		(2.31)	(2.05)	
Z_1	54.91			36.62			18.97		
	(2.65)			(3.35)			(2.27)		
Z_2	98.21			47.43			12.72		
	(2.49)			(2.24)			(0.63)		
$i^* - i$			0.26			-3.32			-2.38
			(0.05)			(-0.78)			(-0.47)
$\bar{R}^2$ (in %)	0.36	0.05	-0.03	5.44	1.99	-0.37	4.37	4.38	-1.55

Table 2: **FX risk premium and yield factors**

This table reports results to the following regression model

$$\eta_t^{BM2} \quad = \quad \alpha + \beta' X_t + \varphi' Z_t + \varepsilon_t,$$

where η_t^{BM2} refers to the model-implied FX risk premium obtained from a model where the short rate differential is the only factor used to explain exchange rate dynamics (as outlined in Section 7.2), X_t contains nominal yield factors, and Z_t contains factors measuring the cross-section of inflation swaps. In the column BM1 (i.e., benchmark model 1), $\varphi = 0$ is restricted to be zero. Results are presented for data sampled at daily, monthly and quarterly frequencies. Numbers in parentheses refer to t-statistics based on Newey-West standard errors. The sample period is from May 8, 2008, to February 5, 2021.

	Daily		Monthly		Quarterly	
	Full	BM1	Full	BM1	Full	BM1
α	0.00	0.00	0.00	0.00	0.01	0.01
	(10.95)	(7.51)	(5.28)	(3.39)	(4.30)	(2.66)
X_1	-3.71	-2.28	-3.88	-2.35	-3.91	-2.29
	(-5.05)	(-2.59)	(-3.16)	(-1.59)	(-2.64)	(-1.24)
X_2	-5.99	-4.36	-6.05	-4.44	-6.01	-4.40
	(-19.79)	(-12.46)	(-11.70)	(-7.43)	(-10.02)	(-6.25)
X_3	-1.06	-1.36	-1.09	-1.36	-1.12	-1.38
	(-8.53)	(-7.96)	(-3.94)	(-3.52)	(-3.30)	(-2.84)
Z_1	-2.85		-2.63		-2.45	
	(-4.20)		(-1.57)		(-1.19)	
Z_2	1.46		2.23		2.83	
	(1.00)		(0.97)		(1.19)	
$\bar{R}^2$ (in %)	86.17	74.67	86.73	76.04	86.14	76.34

Table 3: **Correlation matrix: 2- and 10-year horizons**

This table reports correlation coefficients between the model factors (X_1, X_2, X_3, Z_1, Z_2, η), the observed real exchange rate (q), the model-implied components of the real exchange rate decomposition and the short-term interest rate differential ($i^* - i$). The notation $\hat{x}^m$ denotes the difference in yields with maturity m, e.g., $\hat{x}^m = (x^{m*} - x^m)$. In the top (bottom) panel, the differential is based on interest rates with maturity of 2 years (10 years). The sample period is from May 8, 2008, to February 5, 2021.

Panel A: 2-year maturity

	X_1	X_2	X_3	Z_1	Z_2	η	q_t	$E_t[q_{t+m}]$	$E_t[\hat{\pi}^m]$	$E_t\left[\hat{i}^m\right]$	$\hat{y}^m$	$\hat{TP}^m$	$E_t[r_t]$	$i^* - i$
X_1	1.00													
X_2	-0.82	1.00												
X_3	-0.82	0.59	1.00											
Z_1	-0.13	0.12	0.03	1.00										
Z_2	0.16	-0.14	-0.03	-0.45	1.00									
η	0.76	-0.83	-0.75	-0.24	0.08	1.00								
q	-0.73	0.90	0.63	0.19	-0.16	-0.97	1.00							
$E_t[q_{t+m}]$	-0.78	0.84	0.77	0.23	-0.09	-1.00	0.97	1.00						
$E_t[\hat{\pi}^m]$	-0.29	0.09	0.77	-0.24	0.23	-0.32	0.17	0.34	1.00					
$E_t\left[\hat{i}^m\right]$	-0.76	0.95	0.68	0.22	-0.17	-0.93	0.96	0.94	0.25	1.00				
$\hat{y}^m$	-0.52	0.87	0.52	0.03	-0.04	-0.79	0.86	0.80	0.28	0.93	1.00			
$\hat{TP}^m$	0.04	0.45	0.09	-0.30	0.20	-0.29	0.39	0.30	0.24	0.50	0.79	1.00		
$E_t[r_t]$	0.73	-0.89	-0.68	-0.12	0.14	0.97	-0.99	-0.97	-0.26	-0.97	-0.88	-0.44	1.00	
$i^* - i$	-0.28	0.78	0.13	0.05	-0.06	-0.58	0.72	0.58	-0.12	0.78	0.90	0.81	-0.71	1.00

Panel B: 10-year maturity

	X_1	X_2	X_3	Z_1	Z_2	η	q_t	$E_t[q_{t+m}]$	$E_t[\hat{\pi}^m]$	$E_t\left[\hat{i}^m\right]$	$\hat{y}^m$	$\hat{TP}^m$	$E_t[r_t]$	$i^* - i$
X_1	1.00													
X_2	-0.82	1.00												
X_3	-0.82	0.59	1.00											
Z_1	-0.13	0.12	0.03	1.00										
Z_2	0.16	-0.14	-0.03	-0.45	1.00									
η	0.76	-0.83	-0.75	-0.24	0.08	1.00								
q	-0.73	0.90	0.63	0.19	-0.16	-0.97	1.00							
$E_t[q_{t+m}]$	-0.77	0.83	0.76	0.24	-0.08	-1.00	0.97	1.00						
$E_t[\hat{\pi}^m]$	-0.40	0.21	0.84	-0.20	0.19	-0.43	0.28	0.44	1.00					
$E_t\left[\hat{i}^m\right]$	-0.79	0.93	0.73	0.22	-0.15	-0.96	0.97	0.96	0.41	1.00				
$\hat{y}^m$	-0.44	0.55	0.78	-0.06	0.07	-0.72	0.66	0.73	0.83	0.75	1.00			
$\hat{TP}^m$	-0.28	0.37	0.71	-0.14	0.13	-0.57	0.49	0.57	0.88	0.58	0.98	1.00		
$E_t[r_t]$	0.75	-0.88	-0.71	-0.15	0.13	0.98	-0.99	-0.98	-0.39	-0.98	-0.73	-0.58	1.00	
$i^* - i$	-0.28	0.78	0.13	0.05	-0.06	-0.58	0.72	0.58	-0.03	0.72	0.49	0.36	-0.68	1.00

Table 4: **Summary statistics**

This table reports summary statistics for the daily levels of model-implied components of the real exchange rate decomposition. The row "H(ρ)" refers to the half-life, where ρ refers to an AR(1) coefficient. Panel A (Panel B) refers to model-implied components with a maturity of 2 years (10 years). The notation $\hat{x}^m$ denotes the differential between two country variables, e.g., $\hat{x} = (x^{m*} - x^m)$. In the top (bottom) panel, the differential is based on interest rates with a maturity of 2 years (10 years). The sample period is from May 8, 2008, to February 5, 2021.

Panel A: 2-year maturity							
	q_t	$E_t[q_{t+m}]$	$E_t[\hat{\pi}^m]$	$E_t\left[\hat{i}^m\right]$	$\hat{y}^m$	$\hat{TP}^m$	$E_t[r_t]$
mean	-0.79	-0.79	0.04	0.01	0.00	0.00	-0.04
std	0.12	0.03	0.01	0.01	0.01	0.00	0.09
min	-1.01	-0.85	0.00	0.00	-0.02	-0.01	-0.19
max	-0.57	-0.73	0.08	0.02	0.03	0.02	0.13
skew	0.15	0.24	-0.45	0.27	-0.13	0.05	-0.16
kurt	1.42	1.56	2.49	1.65	1.80	3.14	1.44
$H(\rho)$	531.22	359.64	88.25	670.51	382.31	131.38	508.11
Panel B: 10-year maturity							
	q_t	$E_t[q_{t+m}]$	$E_t[\hat{\pi}^m]$	$E_t\left[\hat{i}^m\right]$	$\hat{y}^m$	$\hat{TP}^m$	$E_t[r_t]$
mean	-0.79	-0.79	0.22	0.03	-0.03	-0.06	-0.19
std	0.12	0.00	0.02	0.01	0.04	0.03	0.12
min	-1.01	-0.79	0.18	0.01	-0.13	-0.15	-0.40
max	-0.57	-0.79	0.25	0.05	0.08	0.05	0.03
skew	0.15	0.21	-0.53	0.32	-0.21	-0.15	-0.18
kurt	1.42	1.56	2.45	1.62	2.05	2.31	1.45
$H(\rho)$	531.22	324.49	94.41	688.19	150.74	112.56	513.37

Table 5: **Monetary policy shock: 2- and 10- year maturities**

This table reports regression results to the model

$$\Delta y_t = c + \beta_1 LEV_t + \beta_2 SLP_t + \varepsilon_t,$$

where Δy_t refers to the daily change between day $t-1$ and day t of the real exchange rate and its individual components, i.e., $y_t \in \{q_t, E\left[q_{t+m}\right]\hat{\pi}, \hat{i}, \hat{y}, \hat{TP}, E_t[r_t]\}$, and where $\hat{x}$ denotes the differential between two country variables, e.g., $\hat{x} = (x^{m*} - x^m)$. LEV denotes the level factor, which is defined as the difference between the median short-term (1-month/3-month) BAX futures rate before and after each monetary policy announcement. SLP denotes the slope factor, which is defined as the difference between changes in the median long-term (13-month/15-month) and short-term (1-month/3-month) BAX rates before and after each monetary policy announcement. Median rates are based on BAX futures rates from 25 to 15 minutes before and from 10 to 20 minutes after an announcement. Summary statistics of the level and slope shocks (in basis points) are shown in Panel A. Regression results for interest rate differentials with a maturity of 2 years (10 years) are shown in Panel B (Panel C). We consider only monetary policy announcement days on which prices for short- and long-term futures contracts are available. Numbers in parentheses refer to t-statistics. The sample period is from May 8, 2008, to February 5, 2021.

Panel A: monetary policy shocks–summary statistics

	N	mean	std	min	Q25	Q50	Q75	max
	count	mean	sd	min	p25	p50	p75	max
LEV	67	-0.79	5.55	-27.25	-2.50	0.00	1.50	11.25
SLP	67	-0.14	2.89	-8.75	-1.50	0.00	1.50	7.00
N	67							

Panel B: regression results–2-years

	$\Delta E_t \Delta q_{t+m}$	Δq_t	$\Delta E_t\left[q_{t+m}\right]$	$\Delta E_t\left[\hat{\pi}\right]$	$\Delta E_t\left[\hat{i}\right]$	$\Delta\hat{y}$	$\Delta\hat{TP}$	$\Delta E_t\left[r_t\right]$
c	-0.51	1.34	0.82	2.15	-0.17	-0.09	0.07	-2.83
	(-0.08)	(0.16)	(0.29)	(1.06)	(-0.39)	(-0.11)	(0.12)	(-0.45)
LEV	-5.17	7.10	1.93	1.56	0.65	1.31	0.66	-6.09
	(-4.57)	(4.67)	(3.78)	(4.26)	(8.35)	(8.28)	(6.09)	(-5.32)
SLP	-7.42	11.51	4.08	2.84	0.47	0.52	0.05	-9.78
	(-3.42)	(3.95)	(4.17)	(4.04)	(3.20)	(1.72)	(0.22)	(-4.46)
adj-R_2	0.34	0.38	0.34	0.36	0.56	0.53	0.35	0.44
Obs	67	67	67	67	67	67	67	67

Panel C: regression results–10-years

	$\Delta E_t \Delta q_{t+m}$	Δq_t	$\Delta E_t\left[q_{t+m}\right]$	$\Delta E_t\left[\hat{\pi}\right]$	$\Delta E_t\left[\hat{i}\right]$	$\Delta\hat{y}$	$\Delta\hat{TP}$	$\Delta E_t\left[r_t\right]$
c	-1.33	1.34	0.00	2.09	-0.13	5.54	5.67	-3.55
	(-0.16)	(0.16)	(0.33)	(0.97)	(-0.19)	(1.30)	(1.46)	(-0.41)
LEV	-7.10	7.10	0.00	1.75	0.89	5.67	4.78	-7.95
	(-4.67)	(4.67)	(3.47)	(4.49)	(7.60)	(7.38)	(6.81)	(-5.12)
SLP	-11.50	11.51	0.01	3.08	0.93	6.76	5.83	-13.65
	(-3.95)	(3.95)	(4.06)	(4.13)	(4.12)	(4.59)	(4.33)	(-4.58)
adj-R_2	0.38	0.38	0.31	0.38	0.55	0.55	0.52	0.44
Obs	67	67	67	67	67	67	67	67

Table 6: **FX risk premium and inflation differential across maturities**

This table reports regression results to the model

$$\Delta y_t = c + \beta_1 LEV_t + \beta_2 SLP_t + \varepsilon_t,$$

where Δy_t refers to the daily change between day $t-1$ and day t of the exchange rate risk premium, $E_t[r_t]$ (Panel A), or the inflation differential, $E_t[\hat{\pi}]$ (Panel B), and where $\hat{\pi}$ denotes the differential between two country variables, e.g., $\hat{\pi} = (\pi^{m*} - \pi^m)$. LEV denotes the level factor, which is defined as the difference between the median short-term (1-month/3-month) BAX futures rate before and after each monetary policy announcement. SLP denotes the slope factor, which is defined as the difference between changes in the median long-term (13-month/15-month) and short-term (1-month/3-month) BAX rates before and after each monetary policy announcement. Median rates are based on BAX futures rates from 25 to 15 minutes before and from 10 to 20 minutes after an announcement. Results for interest rates with different maturities ranging between 3 months ($3M$) and 10 years (30Y) are reported. We consider only monetary policy announcement days on which prices for short- and long-term futures contracts are available. Numbers in parentheses refer to t-statistics. The sample period is from May 8, 2008, to February 5, 2021.

Panel A: FX risk premium									
	3M	6M	1Y	2Y	5Y	10Y	15Y	20Y	30Y
c	-0.97	-1.33	-2.07	-2.83	-3.47	-3.55	-3.56	-3.56	-3.56
	(-0.32)	(-0.39)	(-0.47)	(-0.45)	(-0.42)	(-0.41)	(-0.41)	(-0.41)	(-0.41)
LEV	-0.92	-2.17	-4.02	-6.09	-7.76	-7.95	-7.96	-7.96	-7.96
	(-1.70)	(-3.50)	(-5.02)	(-5.32)	(-5.15)	(-5.12)	(-5.12)	(-5.12)	(-5.12)
SLP	-0.86	-2.79	-5.89	-9.78	-13.24	-13.65	-13.66	-13.66	-13.66
	(-0.83)	(-2.34)	(-3.84)	(-4.46)	(-4.58)	(-4.58)	(-4.58)	(-4.58)	(-4.58)
adj-R_2	0.03	0.21	0.39	0.44	0.44	0.44	0.44	0.44	0.44
Obs	67	67	67	67	67	67	67	67	67
Panel B: inflation differential									
	3M	6M	1Y	2Y	5Y	10Y	15Y	20Y	30Y
c	1.28	1.90	2.19	2.15	2.09	2.09	2.09	2.09	2.09
	(0.98)	(1.15)	(1.15)	(1.06)	(0.98)	(0.97)	(0.97)	(0.97)	(0.97)
LEV	0.78	1.09	1.37	1.56	1.72	1.75	1.75	1.75	1.75
	(3.31)	(3.66)	(3.99)	(4.26)	(4.47)	(4.49)	(4.49)	(4.49)	(4.49)
SLP	1.61	2.20	2.64	2.84	3.03	3.08	3.08	3.08	3.08
	(3.56)	(3.84)	(4.01)	(4.04)	(4.11)	(4.13)	(4.13)	(4.13)	(4.13)
adj-R_2	0.27	0.31	0.34	0.36	0.37	0.38	0.38	0.38	0.38
Obs	67	67	67	67	67	67	67	67	67

Table 7: **Goodness-of-fit: Canadian macroeconomic news surprises**

This table reports results of the regression

$$\Delta^f y_t^\tau = \gamma^{f,\tau} nix^{f,\tau} + \nu_t^{f,\tau},$$

where the regression coefficient $\gamma^{f,\tau}$ measures the impact of the aggregated news surprises on the change in the expected appreciation ($\Delta E_t \Delta q_{t+m}$), in the real exchange rate (Δq_t), in the expected inflation differential ($\Delta E_t[\hat{\pi}]$), or in the FX risk premium ($\Delta E_t[r_t]$), at the monthly (Panel A, $f = M$) or quarterly (Panel B, $f = Q$) frequency, respectively. For both sample frequencies, results are reported for maturities $\tau = 2Y$ (2 years) and $\tau = 10Y$ (10 years). Numbers in parentheses denote t-statistics, based on Newey-West adjusted standard errors. Only Canadian news surprises are considered. The sample period is from May 8, 2008, to February 5, 2021.

Panel A: monthly frequency					
	τ	$\Delta E_t \Delta q_{t+m}$	Δq_t	$\Delta E_t[\hat{\pi}]$	$\Delta E_t[r_t]$
γ^M	2Y	0.56	0.95	0.54	1.01
		(0.91)	(1.68)	(0.83)	(1.37)
	10Y	0.95	0.95	0.56	1.29
		(1.68)	(1.68)	(0.90)	(2.01)
$\bar{R}^2_M$ (in %)	2Y	0.90	2.15	1.25	2.30
	10Y	2.15	2.15	1.32	3.52
Panel B: quarterly frequency					
	τ	$\Delta E_t \Delta q_{t+m}$	Δq_t	$\Delta E_t[\hat{\pi}]$	$\Delta E_t[r_t]$
γ^Q	2Y	1.67	1.78	0.25	1.85
		(3.34)	(3.62)	(0.41)	(3.61)
	10Y	1.78	1.78	0.20	1.75
		(3.62)	(3.62)	(0.34)	(3.19)
$\bar{R}^2_Q$ (in %)	2Y	10.73	11.96	0.38	12.82
	10Y	11.95	11.96	0.28	11.79

Table 8: **Goodness-of-fit: global and Local macroeconomic news surprises**

This table reports results of the regression

$$\Delta^f y_t^\tau = \delta_{CA}^{f,\tau} nix_{CA}^{f,\tau} + \delta_{US}^{f,\tau} nix_{US}^{f,\tau} + \mu_t^{f,\tau},$$

where the regression coefficients $\delta_{CA}^{f,\tau}$ and $\delta_{US}^{f,\tau}$ measure the impact of the aggregated Canadian and US news surprises on the change in the expected appreciation ($\Delta E_t \Delta q_{t+m}$), in the real exchange rate (Δq_t), in the expected inflation differential ($\Delta E_t[\hat{\pi}]$), or in the the FX risk premium ($\Delta E_t[r_t]$), at the monthly (Panel A, $f = M$) or quarterly (Panel B, $f = Q$) frequency, respectively. For both sample frequencies, results are reported for maturities $\tau = 2Y$ (2 years) and $\tau = 10Y$ (10 years). Numbers in parentheses denote t-statistics, based on Newey-West adjusted standard errors. Canadian and US news surprises are considered. The sample period is from May 8, 2008, to February 5, 2021.

Panel A: monthly frequency					
	τ	$\Delta E_t \Delta q_{t+m}$	Δq_t	$\Delta E_t[\hat{\pi}]$	$\Delta E_t[r_t]$
δ_{CA}^M	2Y	0.31	0.82	0.37	0.91
		(0.51)	(1.48)	(0.68)	(1.27)
	10Y	0.82	0.82	0.41	1.24
		(1.48)	(1.48)	(0.77)	(1.98)
δ_{US}^M	2Y	0.93	0.62	0.95	0.48
		(2.86)	(1.99)	(3.48)	(1.65)
	10Y	0.62	0.62	0.92	0.34
		(2.00)	(1.99)	(3.49)	(1.20)
$\bar{R}_M^2$ (in %)	2Y	4.15	3.10	10.28	2.72
	10Y	3.10	3.10	9.42	3.39
Panel B: quarterly frequency					
	τ	$\Delta E_t \Delta q_{t+m}$	Δq_t	$\Delta E_t[\hat{\pi}]$	$\Delta E_t[r_t]$
δ_{CA}^Q	2Y	1.40	1.76	0.08	1.85
		(2.68)	(3.56)	(0.12)	(3.60)
	10Y	1.76	1.76	0.07	1.74
		(3.56)	(3.56)	(0.11)	(3.09)
δ_{US}^Q	2Y	1.04	0.17	0.70	0.13
		(1.52)	(0.32)	(2.26)	(0.25)
	10Y	0.17	0.17	0.61	-0.37
		(0.32)	(0.32)	(2.10)	(-0.55)
$\bar{R}_Q^2$ (in %)	2Y	12.76	10.30	6.73	11.15
	10Y	10.30	10.30	4.84	10.67

References

Altavilla, C., D. Giannone and M. Modugno. 2017. "Low Frequency Effects of Macroeconomic News on Government Bond Yields." *Journal of Monetary Economics* 92 (C): 31–46.

Backus, D. K., S. Foresi and C. I. Telmer. 2001. "Affine Term Structure Models and the Forward Premium Anomaly." *The Journal of Finance* 56 (1): 279–304.

Chen, Y.-C. and K. P. Tsang. 2013. "What Does the Yield Curve Tell Us about Exchange Rate Predictability?" *The Review of Economics and Statistics* 95 (1): 185–205.

Chinn, M. D. and G. Meredith. 2004. "Monetary Policy and Long-Horizon Uncovered Interest Parity." *IMF Staff Papers* 51 (3), 409–30.

Dahlquist, M. and J. Pénasse. 2022. "The Missing Risk Premium in Exchange Rates." *Journal of Financial Economics* 143 (2): 697–715.

Engel, C. 1996. "The Forward Discount Anomaly and the Risk Premium: A Survey of Recent Evidence." *Journal of Empirical Finance* 3 (2): 123–92.

Engel, C. 2013. "Exchange Rates and Interest Parity." National Bureau of Economic Research Working Paper No. 19336.

Engel, C. and K. D. West. 2005. "Exchange Rates and Fundamentals." *The Journal of Political Economy* 113 (3): 485– 517.

Fama, E. F. 1984a. "Term Premiums in Bond Returns." *Journal of Financial Economics* 13 (4): 529–46.

Fama, E. F. 1984b. "Forward and Spot Exchange Rates." *Journal of Monetary Economics* 14 (3): 319–38.

Farhi, E. and X. Gabaix. 2015. "Rare Disasters and Exchange Rates." *The Quarterly Journal of Economics* 131 (1): 1– 52.

Meese, R. A. and K. Rogoff. 1983. "Empirical Exchange Rate Models of the Seventies: Do They Fit out of Sample?" *Journal of International Economics* 14 (1): 3–24.

Nelson, C. and A. F. Siegel. 1987. "Parsimonious Modeling of Yield Curves." *The Journal of Business* 60 (4): 473–89.

Verdelhan, A. 2010. "A Habit-Based Explanation of the Exchange Rate Risk Premium." *The Journal of Finance* 65 (1): 123–46.